

# 1 Tangible and intangible ex-post assessment of flood-induced 2 damages to cultural heritage

3 Claudia De Lucia, Michele Amaddii, Chiara Arrighi

4 Department of Civil and Environmental Engineering, Università degli Studi di Firenze, Via di S. Marta 3, 50139,  
5 Florence, Italy

6 *Correspondence to:* Chiara Arrighi (chiara.arrighi@unifi.it)

7 **Abstract.** Floods pose significant risks to cultural heritage (CH), yet post-disaster damage data to CH remain lacking. In  
8 this paper, we address this gap by focusing on the ex-post assessment of flood-induced damage to CH. The method  
9 involves the identification of damaged assets, and a field survey to assess tangible (LTV) and intangible (LIV) damage.  
10 The potential contributing factors e.g., water depth and river slope, are analyzed through geospatial analysis. Ex-post  
11 damage data to CH are compared with the outcome of an ex-ante analysis based on available methods to verify the quality  
12 of exposed data and possible limitations. The method is applied to the 15-16 September 2022 flood event that occurred  
13 in the Marche Region (Italy). The survey involved 14 CH in 4 municipalities and 3 catchments. Results highlight the  
14 inadequacy of existing exposure data for ex-ante damage assessment [and the importance of building characteristics](#).  
15 However, ex-post data confirm that religious architectures are likely to suffer the highest LTV and LIV. The ex-post  
16 damage analysis provided a semi-quantitative evaluation of both LTV and LIV in relation to flood characteristics.  
17 Notably, significant correlations between LTV and flood depth, as well as with the slope of the riverbed (a proxy for river  
18 flow velocity), were found. LIV correlates well to flood depth and river slope although with lower  $R^2$  and larger RMSE,  
19 highlighting that intangible impact analysis requires more effort than hazard characterization. Further research should  
20 increase the availability of ex-post damage data to CH to pose the basis for damage model validation and development of  
21 empirical vulnerability functions.

## 22 1 Introduction

23 Floods are among the most frequent and costliest natural hazards (CRED [and UNISDR, 2015](#)). In recent decades, the  
24 frequency and intensity of heavy rainfall, associated with ongoing climate change have consequently led to an increase  
25 in flood events (Merz et al., 2021; IPCC, 2023). Moreover, due to severe urbanization and increasing development in  
26 flood-prone areas, flood impacts are expected to grow in the future (Dottori et al., 2023).

27 The EU Flood Directive calls upon member countries to mitigate the potential adverse consequences of flooding on  
28 human health, the environment, cultural heritage, and economic activities (EU Flood Directive, 2007/60/EC). Concerning  
29 cultural heritage (CH), this purpose gains even more significance. Indeed, CH assets are severely affected by floods and  
30 are likely to be increasingly threatened by climate change effects (Marzeion and Levermann, 2014; Fatoric and Seekamp,  
31 2017; Sesana et al., 2021). In many cases, substantial costs for restoration are necessary, and in the worst-case scenario,  
32 the irreversible destruction of unique and irreplaceable assets that hold cultural significance is unavoidable (Arrighi, 2021;  
33 Arrighi et al., 2023b). Furthermore, the impact of floods on CH extends beyond the tangible damage, affecting social  
34 identity and cohesion (Romão et al., 2020).

35 Cultural heritage can be defined as the legacy of tangible and intangible attributes inherited from past generations.  
36 Tangible attributes include buildings, monuments, and historic places, as well as works of art, literature, music, and  
37 artifacts both archaeological and historical. Intangible attributes comprise social customs, traditions, and practices, rooted  
38 in aesthetic and spiritual beliefs and oral traditions (Willis, 2014).

ha eliminato: , 2015;

ha eliminato: Wallemacq et al., 2015

41 Over the past decades, ex-ante damage assessment, namely impact analysis and mitigation measures of natural hazards  
42 to CH assets, such as floods, received considerable scientific attention. Many researchers focused on individual assets or  
43 site levels (Sabbioni et al., 2006; Drdácý, 2010; Huijbregts et al., 2014; [Figueiredo et al., 2021](#); Sesana et al., 2021;  
44 Momčilović Petronijević and Petronijević, 2022; Anderson, 2023). Other studies focused on the negative effects of natural  
45 hazards on CH concerning societal impacts and economic losses (Alexandrakis et al., 2019; Garrote et al., 2020).  
46 Additionally, several studies have focused on flood risk assessment of CH at various scales, ranging from specific sites  
47 ([Zhang et al., 2024](#)), to cities (Wang, 2015; Arrighi et al., 2018; Trizio et al., 2021; Schlumberger et al., 2022; Arrighi et  
48 al., 2023a; Brokerhof et al., 2023; Ravan et al., 2023), regions (Godfrey et al., 2015; Figueiredo et al., 2020; [Garrote et  
49 al., 2020](#); Arrighi et al., 2023b), national levels (Stephenson and D’Ayala, 2014), and even globally (Reimann et al., 2018;  
50 Arrighi, 2021). The ex-ante analyses represent a key aspect of any "flood risk management plan", as required by the EU  
51 Flood Directive (EU Flood Directive, 2007/60/EC). However, estimating the loss after an event is equally important to  
52 support emergency management and decide priorities for reconstruction and victim compensation (Molinari et al., 2014).  
53 Furthermore, identifying key factors influencing the vulnerability of CH assets is necessary for a more robust risk  
54 assessment. Achieving this requires the availability of post-disaster loss information and data, coupled with appropriate  
55 ex-post damage analyses. Such endeavours would highlight weaknesses in current risk management practices and thus  
56 improve the effectiveness of preparedness and resilience strategies (Arrighi et al., 2022). Nevertheless, there are only a  
57 few examples in the literature concerning the ex-post assessment of damage to CH. In the work of Vecvagars (2006), an  
58 overview of the different available methods in assessing the value of CH assets, providing some recommendations for  
59 valuing damages and losses after a disaster, is outlined. Since 2008, the European Commission, the United Nations  
60 Development Group, and the World Bank developed the joint Post-Disaster Needs Assessment (PDNA) tool. This tool  
61 provides a comprehensive, government-led assessment of post-disaster damages, losses, and recovery needs, paving the  
62 way for a consolidated recovery framework. The PDNA framework encompasses the gathering of data on damages to  
63 both tangible and intangible values of cultural assets. More recently, a reviewed version of the PDNA, based on  
64 experiences gathered through the analysis of many PDNA post-disaster assessments conducted since 2008, was published  
65 (Jeggle and Boggero, 2018). Vafadari (2017) developed a tool for the recording and inventory of sites and monuments as  
66 well as to record damage and threats, their causes, and assess their magnitude. Deschaux (2017) details the observed  
67 impacts on movable and immovable heritage following the floods in Central France in 2016. Figueiredo et al. (2021)  
68 analyze the impacts of wildfires that occurred in Portugal on cultural heritage integrating geospatial analysis with  
69 information provided directly by municipalities affected by the wildfires.

70 As already mentioned, CH assets are characterized by both tangible and intangible value, and consequently, the damage  
71 they suffer can be tangible and intangible. Therefore, for an adequate assessment of flood damage to CH, a classification  
72 of these values is necessary (Romao et al., 2020), whether the analysis is conducted ex-ante or ex-post. Vecvagars (2006)  
73 groups cultural heritage values into "use value" (related to market value) and "non-use value" (i.e., non-market value such  
74 as spiritual value, legacy value, and social value). In addition, use value can be further divided into "extractive use value"  
75 and "non-extractive use value". Extractive use value includes consumptive value, which can be measured through market  
76 transactions. Non-extractive use value originates from the service the asset provides and includes aesthetic and  
77 recreational values.

78 However, it is often noted that quantitative disaster data concerning losses related to cultural heritage are either scarce or  
79 entirely unavailable (Romão et al., 2020). This underscores the persistent challenges in obtaining comprehensive  
80 information on the impact of disasters on cultural heritage, emphasizing the need for improved data collection and  
81 assessment methodologies in this critical domain, which are essential for damage model calibration and validation.

ha eliminato: Garrote et al., 2019;

83 This paper focuses on the analysis of damage to CH assets as a consequence of a flood event. First, an ex-ante analysis  
84 was performed using the available data. The official existing hydraulic hazard maps and the national CH database were  
85 considered. However, the pivotal aspect of this study lies in the ex-post damage assessment. A well-defined workflow  
86 has been proposed to assess the tangible and intangible losses incurred by CH due to flooding: (i) identification of the  
87 assets potentially damaged by the flood; (ii) field data collection for the assessment of damage to CH; (iii) ex-post damage  
88 assessment considering both tangible and intangible values of the damaged assets; (iv) analysis of the possible  
89 contributing factor of the damage to CH.

90 The proposed method is applied to the case study of the flood event that impacted the Marche Region (Central Italy) on  
91 15-16 September 2022. The involved sites encompass different types of assets such as churches, historic bridges, and  
92 industrial buildings, which are located in three basins in the Marche region: Burano, Cesano, and Misa.

93 Through the method proposed in this paper, we aim to fill the gap in the literature concerning ex-post assessment of  
94 cultural heritage damage induced by floods. The research pinpoints the factors that significantly contribute to the  
95 vulnerability of cultural heritage and the resulting flood-related damages.

## 96 2 Materials and methods

97 This section outlines the evaluation of flood damage to CH assets using two approaches: ex-ante and ex-post. Sect. 2.1  
98 details the ex-ante damage analysis, which was conducted using available data. On the other hand, Sect. 2.2, the focus of  
99 the paper, describes the procedure for the ex-post damage assessment.

### 100 2.1 Ex-ante damage assessment

101 The aim of the ex-ante damage assessment is to investigate if using the available data before the flood event, it would  
102 have been possible to predict the degree of flood damage to CH. The database of CH considered for this analysis consists  
103 of the assets included in the national MIC database (Istituto Superiore per la Conservazione ed il Restauro – MiBACT,  
104 2024). The database contains movable and immovable assets under protection with declared cultural interest of national  
105 level of listing as well as UNESCO sites. In addition, it includes assets older than 50 or 70 years under evaluation to  
106 verify their effective cultural interest (D.lgs. 22 gennaio 2004, n. 42). The assets that overlap with the official map of  
107 flood hazard areas are then considered. The ex-ante damage assessment was evaluated as the combination of exposure  
108 and vulnerability (Arrighi et al., 2023b).

109 Exposure of CH can be evaluated by intersecting the shapefile of CH with the official flood hazard map available from  
110 the website of the competent authority (AUBAC, 2024). As the MIC database does not provide information about CH  
111 value, and assets of regional or local listing are not included, an exposure score equal to 1 ( $E = 1$ ) is assigned to all assets  
112 that overlay areas with some probability of inundation (i.e., P3 – high probability; P2 – medium probability; P1 – low  
113 probability). On the other hand, a 0 score is attributed to all those assets that are not potentially flooded.

114 According to the vulnerability classification of Arrighi et al. (2023b), a vulnerability class is defined for each CH based  
115 on its typology.

- 116 - Very high vulnerability: religious, residential, tertiary, fortified architectures, and museums.
- 117 - High vulnerability: industrial, productive, rural architectures, and monuments.
- 118 - Medium vulnerability: archaeological areas, infrastructure, and plants.
- 119 - Low vulnerability: open spaces.

ha eliminato: interested

ha eliminato: the

ha eliminato: of the assets

ha eliminato: only contains items of national

124 According to this approach and based on the available data, considering the same value (E=1) for all assets then results  
125 in damage equal to vulnerability.

## 126 2.2 Ex-post damage assessment: The workflow

127 The proposed workflow consists of 4 steps. The first step is focused on the identification of CH assets actually damaged  
128 by the flood (Sect. 2.2.1). Then, in the second step, a post-event field survey, based on on-site visual inspection, is  
129 conducted to evaluate the actual state and condition of CH assets (Sect. 2.2.2). Once all the data and information on the  
130 damage to CH assets is obtained, the ex-post evaluation can be carried out assigning the intangible value to the assets, as  
131 well as the tangible and intangible losses based on post-event evidence (Sect. 2.2.3). Lastly, the analysis of which factors  
132 contributed most to the damage, by means of geospatial methods, is performed (Sect. 2.2.4).

ha eliminato: the assets both tangible and intangible value

ha eliminato: s

ha eliminato: and

### 133 2.2.1 Identification of CH assets potentially damaged by the flood

134 The initial step is dedicated to identifying CH assets situated within the flooded areas. For the purpose of this paper, CH  
135 refers to immovable and movable assets that hold aesthetic, historical, testimonial, municipal, and touristic value. The  
136 MIC database is considered the source for identifying CH assets that reflect this definition. The data can be downloaded  
137 from the MIC cartographic tool (Istituto Superiore per la Conservazione ed il Restauro – MiBACT, 2024) and  
138 comprehends architectural and archaeological assets, as point features. After the field survey verification, the list of the  
139 assets included in the MIC database could be modified, possibly adding, and also disregarding some assets, as explained  
140 in Sect. 2.2.2. Once the database of CH is obtained, the identification of the assets potentially damaged by the flood is  
141 accomplished through the availability of the map of flooded areas (shapefile format) that is freely available for download  
142 from the Copernicus Emergency Management Service (COPERNICUS Emergency Management Service – Mapping,  
143 2022). The flood map generation is based on the acquisition, processing, and analysis, in rapid mode, of satellite imagery  
144 and other geospatial raster and vector data sources. The identification of potentially damaged assets is obtained by  
145 overlaying the shapefiles of the flooded area and the CH database in a GIS environment. In this way, it is possible to  
146 obtain a database of CH assets affected by a flood event, which contains key information, such as name, type, and geo-  
147 localization of each individuated asset.

ha eliminato: The CH database of MIC could be considered for this analysis.

### 148 2.2.2 Post-event field data collection

149 As mentioned in Sect. 2.2.1, the list of damaged CH was updated after the post-event field data collection. Additional  
150 assets not included in the MIC database but identified as culturally significant by local authorities were considered for  
151 the ex-post damage assessment. On the other hand, the assets listed in the MIC database that are not mentioned by local  
152 authorities and by official tourism websites or have no reviews on major platforms (e.g., TripAdvisor and Google), could  
153 be excluded. Indeed, as described in Sect. 2.1, the MIC database also includes assets older than 70 years, pending  
154 verification of their cultural significance. Consequently, the database may contain many private houses or industrial  
155 structures older than 70 years old that lack cultural significance or tourist interest. However, the completeness of the  
156 damaged CH assets was reviewed in collaboration with local authorities.

ha eliminato: In addition to the CH assets identified as described...

ha eliminato: other assets can be considered and then added to the database based on feedback from local authorities. Indeed, based on the purpose of the work, immovable and movable assets characterized by aesthetic, historical, testimonial, and municipal value, as well as those with tourist or local significance identified by local authorities, are considered.

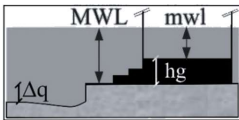
ha eliminato: However

157 A novel procedure for data collection aimed at assessing the damage to CH as a result of flooding has been conceptualized.  
158 The data collection forms implemented by Molinari et al. (2014) for residential buildings and industrial facilities were  
159 modified and adapted to the characteristics of CH. Besides the information about the asset, the flood event (e.g., maximum

175 water level), the presence and typology of any movable artworks, and the observed physical damages, the form allows  
 176 for the registration of the cultural value of the CH. [Table 1](#) summarizes the information collected on the field, through the  
 177 survey form.

178 **Table 1 - Survey form: description of CH assets and aspects considered.**

Form type	CH/flood/damage description	Aspects
General information		
	General features of CH	Geographic coordinates or address CH denomination Level of listing Typology of CH Current use Cultural value Property Fieldworker
	<u>Construction features</u>	Period of construction <u>Type of structure</u> External ornamental elements N° of floors and <u>construction height</u> <u>Presence of basement floors</u> <u>Height of the inside ground floor (hg)</u> <u>Height difference between CH and a flat area (<math>\Delta q</math>)</u>
	<u>Flood characteristics</u>	Duration <u>MWL</u> <u>mwl</u> <u>Sediments grain size or contaminants</u>
	Identification and type of damage	Structural, loss of accessibility Features damaged
<u>Construction internal damage</u>		
	Damage to floors (exposure/vulnerability of the containing <u>construction</u> )	Covered and uncovered surface Level of maintenance Presence and type of plants Damage to frescoes and wall paintings, doors and windows, floors, plants
Contents damage		
	Identification of movable assets	Presence and type of artworks
	Damage to the artworks (exposure/vulnerability of contents)	Damage to furniture, paintings, sculptures, books, decorative items, votive and liturgical elements, textile, archaeological finds



ha eliminato: Table 1  
 ha formattato: Tipo di carattere: 10 pt, Non Grassetto

ha eliminato: D  
 ha eliminato: of CH

ha eliminato: Building

ha eliminato: Building

ha eliminato: building

ha eliminato: Q

ha eliminato: Max. water level outside the building  
 Max. water level inside the building

ha eliminato: Building

Tabella formattata

ha eliminato: building

Tabella formattata

ha eliminato: TheAmong the most significant values to be measured in the post-event field survey are “hg”, “ $\Delta q$ ”, “MWL”, and “mwl” (diagram in [Table 1](#)). Hg refers to the construction’s elevation, such as ofIndeed, form also reports the measure of “Max. water level outside the building” (see the general information form of [Table 1](#)). This task refers to the on-site evaluation of the maximum height reached by water around the damaged CH assets as a result of the river overflow (hereafter MWL).

ha eliminato: Table 1

ha formattato: Tipo di carattere: 10 pt, Non Grassetto

179 Among the most significant values to be measured in the post-event field survey are “hg”, “ $\Delta q$ ”, “MWL”, and “mwl”  
 180 (diagram in [Table 1](#)). The hg value represents the elevation of the construction, such as the height of the steps leading  
 181 into a religious building. The term  $\Delta q$  indicates the difference in elevation between the ground level outside the considered  
 182 CH asset and a reference point in a flat area. MWL and mwl indicate the maximum water level outside and inside the  
 183 construction, respectively. Concerning the mwl, it could be very different from the MWL depending on variations in hg.

205 When a flooded CH site can be clearly geolocated, it may be sufficient to measure the MWL from the ground floor where  
 206 the asset is located to the mud marks that were still visible at the time of the field survey. If variations in the MWL are  
 207 observed around the perimeter of the structure, multiple measurement points should be recorded, and an average height  
 208 value can then be calculated. This measurement can be done using a traditional meter or a laser distance meter. In cases  
 209 where accurate geo-localization of the CH site is not feasible due to a lack of detailed topographic maps or databases, or  
 210 if the asset is located on uneven terrain with significant elevation changes, a suitable reference point should be selected.  
 211 This reference point should be in a flat area whose coordinates can be easily identifiable on a GIS system. Therefore, the  
 212  $\Delta q$  (diagram of Table 1) can be measured. By adding  $\Delta q$  to the MWL, the maximum water height can then be accurately  
 213 mapped within a GIS system. Practically, an operator, using a laser distance meter, points horizontally from the  
 214 measurement level to the reference level, while another field operator located on the reference point, can measure the  
 215 height of the laser from the ground level.

216 In the case of a levelled bridge, the reference level from which the MWL is measured corresponds to the deck. In contrast,  
 217 for a downward-arched bridge, the reference level should correspond to the intrados, and for an upward-arched bridge, it  
 218 should correspond to the extrados.

219 As concerns the cultural value assignment, the following procedure is adopted. Based on the qualitative descriptors  
 220 introduced by Historic England (2008), non-extractive and non-use values were outlined in four categories: evidential,  
 221 historical, aesthetic, and communal value:

- 222 • Aesthetic value: includes aspects of sensory and intellectual stimulation from the CH.
- 223 • Historical value: derives from the connection between the past and the present through the asset. It includes (i)  
 224 illustrative value if the asset illustrates something unique or rare and (ii) associative value if it is associated with  
 225 a notable family, person, or event.
- 226 • Evidential value: derives from the potential of the asset to yield evidence about past human activity.
- 227 • Communal value: derives from the meanings of a place for the people who relate to it, or for whom it figures in  
 228 their collective experience or memory. It encompasses (i) commemorative value, (ii) social value, and (iii)  
 229 spiritual value.

230 Each category of value can be described by four qualitative levels ranging from unknown or no value to high value: the  
 231 respective “V” score was assigned to each asset. It is noteworthy that the chosen hierarchical system incorporates  
 232 “unknown value” and “no value” levels. Indeed, in case of scarce data, it could be challenging to distinguish between  
 233 sites that lack certain categories of value and assets whose value in those categories is unknown. Table 2 summarizes, for  
 234 each category of value, the criteria to be considered when assessing the level of value of the cultural property and the  
 235 scores corresponding to each class of value.

236 Following Romao and Paupério (2021), the baseline pre-disaster intangible value  $BV$  of a certain CH asset will then  
 237 correspond to the sum of the scores established for each type of value given by:

$$BV = \sum_{i=1}^4 V_i \quad \text{Eq. 1}$$

238 where  $V_i$  is the score of  $i$ th typologies of value.

239 While Romao and Paupério (2021) proposed six classes based also on the level of interest of the asset, the classification  
 240 proposed in this paper required a simplified classification with four value categories. Indeed, the available information

ha eliminato: from

ha eliminato: to the

ha eliminato: or if the asset is located on uneven terrain with significant elevation changes

ha eliminato: Table 1

ha eliminato: reached by the water

ha eliminato: could

ha formattato: Tipo di carattere: Non Grassetto

ha eliminato: be correctly

ha eliminato: Indeed, referring to the measurement of the maximum height reached by the water to a reference level is necessary to correctly locate the data collected on a GIS system. Therefore, the difference in height between the maximum level reached by the water outside the considered CH asset and the reference level is measured.

ha eliminato: HE,

ha eliminato: excludes the

ha eliminato: ,

ha eliminato: preferring to assign an “unknown value” to the asset without evidence that would support its significance

ha eliminato: Table 2

ha formattato: Tipo di carattere: 10 pt, Non Grassetto

ha formattato: Tipo di carattere: 10 pt, Non Grassetto, Non Corsivo

261 does not allow for a more detailed assignment of intangible value classes. Therefore, the scores assigned to the class value  
 262 are independent of the level of listing/protection of the CH assets.

263 Table 2 - Classification and criteria to define intangible value of CH with their respective class and associated score.

Type of value	Criteria to assign CH value	Class value and score (V <sub>i</sub> )
Aesthetic	Valuable structure (e.g., architectural art using local materials or high-value import materials) <u>and</u> valuable artworks inside (objects of outstanding workmanship, precious votive elements)	High (10)
	Valuable structure or valuable artworks	Moderate (7)
	No uncommonly attractive qualities, but that display particular characteristics of an identified style	Limited (3)
	No valuable characteristics or stylistic features	Unknown <u>or no value</u> (0)
Historical	Proved illustrative and associative value or pre- <u>19<sup>th</sup> century</u> structure	High (10)
	<u>19<sup>th</sup> century</u> structure	Moderate (7)
	<u>1<sup>st</sup> mid of 20<sup>th</sup> century</u> structure	Limited (3)
	<u>2<sup>nd</sup> mid of 20<sup>th</sup> century</u> structure	Unknown <u>or no value</u> (0)
Evidential	Physical remains of past human activities. The current use has not deleted proofs of the past	High (10)
	No evidence of the past, but their history is based on past human activity	Moderate (7)
	Only the denomination recalls past human activity	Limited (3)
	No linked to past human activities	Unknown <u>or no value</u> (0)
Communal	Spiritual, social, or commemorative value. Additionally, committees have been founded to promote or defend the asset, or the asset is linked to a specific local tradition	High (10)
	Spiritual, social, or commemorative value. No committees or traditional events are linked to the asset	Moderate (7)
	Limited spiritual value (e.g., place of worship with sporadic openings). No traditional events are linked to the CH	Limited (3)
	No spiritual, social or commemorative value	Unknown <u>or no value</u> (0)

ha eliminato: ;

ha eliminato: 1800

ha eliminato: 1800

ha eliminato: 1900

ha eliminato: Structures under 70 years of age

264 2.2.3 Ex-post damage assessment

265 The level of damage is obtained by combining loss in tangible and in intangible values. Loss in tangible value is strictly  
 266 linked to the observed physical damages caused by the flood. It includes structural and non-structural damage. The Italian  
 267 Civil Protection Department defines structural damage as those involving the load-bearing elements of the building, such  
 268 as walls, arches, pillars, beams, and slabs. In case of non-structural damage, the elements that do not affect the stability  
 269 of the building such as ceiling and floor finishes, plumbing, and electrical systems are affected.

ha eliminato: and to the costs of restoration

276 Concerning the loss in intangible value, this is mainly caused by the direct impact of floods, but also by indirect impacts  
 277 such as mold and moisture, although in a less impactful way. Loss in aesthetic value refers to the effectiveness of  
 278 restoration in allowing the community to be sensorial stimulated by the asset again. The impact on historical and evidential  
 279 values depends on how the flood impacted the original structure and materials or the proofs of past human activities, such  
 280 as plaques or archives. Finally, the loss in communal value is measurable as the duration of inaccessibility of the asset  
 281 (HE, 2008). In general, physical damage can lead to a loss of aesthetic value, and if the damage includes the complete  
 282 destruction of the site, it will result in a total or near-total loss of historical and evidential value. In this paper, we assume  
 283 that an asset sustaining moderate damage may be closed for days or weeks for clean-up and safety check operations,  
 284 whereas an asset with severe damage may be closed for months for restoration works. It is also assumed that if an asset  
 285 remains inaccessible for more than one year the loss in intangible value is comparable to the destruction, as the community  
 286 will move to a new place to express communal value.

287 Damage is categorized into four hierarchical classes, with each asset assigned both a loss in tangible value (LTV) and a  
 288 loss in intangible value (LIV). As reported in Table 3, LTV ranges from 5 to 30. The minimum value is greater than 0 as  
 289 the classification system is designed for those assets actually damaged by the flood, even if only slightly, so that cleaning  
 290 is sufficient to restore them. We assumed a degree of damage that varies linearly for the first three classes, namely “slightly  
 291 damaged” (LTV=5), “moderately damaged” (LTV=10), and “severely damaged” (LTV=15). On the other hand, in the  
 292 case of a “destroyed” asset (LTV=30), the assigned score is double that of the “severely damaged” class. This emphasizes  
 293 the difference between a severely damaged site that can be repaired despite the high cost, and a lost site that cannot be  
 294 restored. Regarding the calculation of LIV, the methodology outlined in Romao and Paupério (2021) is applied. This  
 295 method employs a coefficient  $D_i$  (Table 3), which spans from 0 to 1, associated with each class of loss or damage. Then,  
 296 for each cultural heritage asset, the loss in LIV is defined applying Eq. 2:

$$LIV = \sum_{i=1}^4 V_i \times D_i \quad \text{Eq. 2}$$

297 where  $V_i$  represents the score of the category of values. As shown in Table 2, the score of  $V$  ranges from 0 to 10, while  
 298 the coefficient  $D$  could be at most equal to 1, resulting in a LIV score that ranges from 0 to 40. This implies, therefore,  
 299 that greater weight is given to LIV than to LTV to emphasize the peculiar contribution of intangible aspects to the loss  
 300 evaluation. In contrast to LTV, where the first damage class starts at 5, the first class for LIV can be 0. Indeed, in cases  
 301 where an asset is only muddied without sustaining further damage, no loss of intangible value has occurred, allowing the  
 302 population to continue enjoying its values. All damages classes for LTV and LIV, along with the criteria adopted to define  
 303 the loss scores, considering both tangible and intangible features, are reported in Table 3.

304 Table 3 - Classes of damage and definition of LTV and LIV.

Classes of damage	LTV	LIV
Slightly damaged	CH can return to its original state with deep cleaning.	The intangible values have not been impacted. The site has never been closed off, but the flood has limited the accessibility to the site during the event or in the immediate aftermath.
	LTV=5	D = 0

ha eliminato: On the other hand,  
 ha eliminato: is established by evaluating flood indirect impacts...

ha eliminato: Table 3  
 ha formattato: Tipo di carattere: 10 pt, Non Grassetto  
 ha formattato: Tipo di carattere: 10 pt, Non Grassetto, Non Corsivo

ha eliminato: while calculating  
 ha eliminato: involves applying  
 ha eliminato: (  
 ha eliminato: )  
 ha eliminato: Table 3  
 ha eliminato: ,  
 ha formattato: Tipo di carattere: 10 pt, Non Grassetto

ha formattato: Tipo di carattere: 10 pt, Non Grassetto, Non Corsivo  
 ha eliminato: Table 2  
 ha formattato: Tipo di carattere: 10 pt, Non Grassetto  
 ha formattato: Tipo di carattere: 10 pt, Non Grassetto, Non Corsivo

ha eliminato: The  
 ha eliminato: of  
 ha eliminato: damage  
 ha eliminato: and  
 ha eliminato: Table 3  
 ha formattato: Tipo di carattere: 10 pt, Non Grassetto  
 ha formattato: Tipo di carattere: 10 pt, Non Grassetto, Non Corsivo  
 ha eliminato: Undamaged  
 ha eliminato: or s  
 ha eliminato: but the flood has limited the accessibility to the site during the event or in the immediate aftermath.



Moderately damaged	Slight structural and non-structural damages (door unhinged, appliances damaged, and presence of mold).	Restoration can repair most of the features that provide aesthetic, historic, or evidential value. The site has been closed for days or weeks.
	LTV=10	$D = 0.3$
Severely damaged	Building and artworks damaged (wrecked floor, wall painting, sculptures, paintings, furniture, wooden choir, pipe organ, liturgical supply ruined).	Despite restoration works, the damaged features that hold aesthetic, historical, and evidential significance cannot be fully restored to their original state. The site has been closed for months.
	LTV=15	$D = 0.7$
Destroyed/lost	Asset destroyed (the <u>construction material</u> are not on site anymore).	Lost in significance. The site or its most relevant features are destroyed and/or closed for more than one year.
	LTV=30	$D = 1$

ha eliminato: building  
 ha eliminato: materials

#### 2.2.4 Factors influencing flood damage

Flood damage to constructions can be caused by several factors, both intrinsic, influenced by the properties of the structure itself, and extrinsic, influenced by the dynamics of the flood event. In literature, the following factors are typically considered: intrinsic factors of the construction, such as the built material, the presence of contents susceptible to flood damage and with significant cultural value, the existence of possible water communication between the construction and the river, the presence of defence elements, age in years, number of floors, shape, orientation in respect to the water flow, state of conservation, and objects that drag the sheet of water; extrinsic factors such as maximum water level outside the construction, flow velocity, hydrodynamic pressure, flood duration, presence of sediments, and contaminations (e.g., Smith, 1994; Kreibich and Thieken 2008; Dall’Osso et al., 2009; Dutta et al., 2011; Galasso et al., 2021; Marin Garcia et al., 2023).

ha eliminato: buildings

These factors can be directly assessed by means of post-event field survey, or by the interpretation of post-event photos and videos and can be classified based on the level of difficulty in obtaining them (Marin Garcia et al., 2023).

Additionally, other authors (e.g., Cuca and Barazzetti, 2018; Di Salvo et al., 2018; Kefi et al., 2020; Al-Kindi and Alabri, 2024) also consider some geospatial factors as they could influence constructions damage: difference between the level of the ground floor of the construction and the riverbank, distance from the river, difference between the Digital Terrain Model (DTM) and the filled DTM, local slope, curvature, topographic wetness index (Beven and Kirkby, 1979), stream power index (Moore et al., 1991), terrain ruggedness index (Riley et al., 1999), and NDVI.

ha eliminato: of construction

ha eliminato: building

ha eliminato: of the building

ha eliminato: building

ha eliminato: building

ha eliminato: of the building

ha eliminato: building

The relationship between MWL and structural damage is well-known in the literature. For its evaluation, post-event field survey measurements are necessary (as described in Sect. 2.2.2). On the other hand, the evaluation of the geospatial factors requires the use of source data in vector (e.g., hydrographic network, and constructions) and raster formats such as the Digital Elevation Model (DEM), which are generally available from national or regional databases. Concerning the DEM spatial resolution, the degree of damage to constructions could result from small variations of the morphology. For this reason, the use of high-resolution DEM (cell size ranging between 1×1 m and 5×5 m) is recommended, especially in the case of urban flood analysis (Mark et al., 2004; Adeyemo et al., 2008; Di Salvo et al., 2018).

ha eliminato: buildings

ha eliminato: building

ha eliminato: between

ha eliminato: and building

Specific procedures using GIS tools are implemented to assess two factors: the minimum distance ( $\Delta D$ ) between a CH asset and the river, and the elevation difference ( $\Delta E$ ) between the CH asset and the riverbed. For a more accurate

ha eliminato: buildings

ha eliminato: e.g.,

ha eliminato: buildings

368 [evaluation of some of these factors, it is advisable to rely on the areal extent of the CH asset rather than on a single point.](#)  
369 [In this respect, GIS analysis for the analyzed assets can be conducted using the polygon shapefiles of constructions, which](#)  
370 [are generally available in regional or national databases. If polygonal shapefiles are not available, the shape of the assets](#)  
371 [can be digitalized based on sufficiently detailed topographic maps or aerial photos.](#) For  $\Delta D$ , the centroid of the  
372 [construction](#) polygons is considered, with the river network as the reference for distance evaluation. Using the centroid  
373 of the [constructions](#) and the nearest point on the hydrographic network, the  $\Delta D$  factor is determined automatically with  
374 GIS tools (e.g., the Near tool in Analysis Tools of ESRI™ ArcGIS Pro™). Concerning  $\Delta E$ , for each [construction](#) polygon,  
375 the [median value of the](#) DTM is extracted. The elevation difference between the CH asset [polygon](#) and the nearest point  
376 feature on the riverbed is then calculated. To refine the riverbed elevation, a buffer distance around the riverbed can be  
377 considered.

378 Concerning the river slope factor (RS), we assume that the average slope of the riverbed is a reasonable proxy for the  
379 river flow velocity, which is difficult to estimate in the absence of instrumented sections or video recordings during a  
380 flood. Moreover, the slope of the river also influences the transport of sediment and the grain size, which in turn can affect  
381 the degree of damage. Based on our best knowledge, there are no specific recommendations for RS evaluation in the  
382 literature. In this paper, the average slope of 500 m and 1000 m upstream stretch with respect to the assets, is considered.  
383 Regarding the other geospatial factors, these can be evaluated as indicated by the relevant literature cited above. To  
384 evaluate the relationship between each contributing factor and the tangible and intangible losses, the mean and median  
385 values of the area of each CH asset polygon are considered.

386 [To explore the correlation between LTV and LIV with the contributing factors, both LTV and LIV were normalized](#)  
387 [relative to their maximum values, assigning 1 to represent maximum damage and 0 to represent minimum damage. A](#)  
388 [simple correlation analysis was then performed using a linear model \(Sect. 4.1.2\).](#)

### 389 3 Case study

390 The method is applied to CH assets damaged by the 15-16 September 2022 flood in the Marche Region. This section  
391 includes an overview of the basins, along with a general description of the municipalities and their historical significance  
392 (Sect. 3.1). Moreover, the dynamics of the intense rainfall event and associated flooding are described in Sect. 3.2.

393 The geospatial data utilized for the analyses outlined in Sect. 2.2 were sourced from official regional and national  
394 databases. Vector data ([such as buildings and river network](#)) and the numerical technical map of the Marche Region  
395 ("CTR", scale 1:10000) were obtained freely from the Marche regional cartographic data portal (REGIONE MARCHE,  
396 Ambiente, 2023). The LiDAR-derived DEM, with a spatial resolution of 1 m and vertical accuracy of 0.15 m (comprising  
397 both DSM and DTM data), was acquired following a request to the Italian Government's "Ministero dell'Ambiente e della  
398 Sicurezza Energetica" (MASE, Geoportale Nazionale, 2024). Specifically for the coastal area of Senigallia, a portion of  
399 the LiDAR data utilized had a spatial resolution of 2x2 meters.

#### 400 3.1 Overview of the study areas

401 The CH assets damaged by the flood are distributed across three basins on the eastern slope of the Central Apennine chain  
402 of the Marche Region, in Central Italy ([Fig. 1a, b](#)). The basins are drained by their respective main rivers, namely Burano  
403 (a right tributary of the Metauro River), Cesano, and Misa ([Fig. 1b](#)). The highest peak of the study area, Mt. Catria (1704  
404 m a.s.l.), is situated at the watershed between the Burano and Cesano basins. The highest peak of the Misa basin  
405 corresponds to Mt. Sassone, reaching an elevation of 826 m a.s.l. ([Fig. 1b](#)).

ha eliminato: building

ha eliminato: buildings

ha eliminato: building

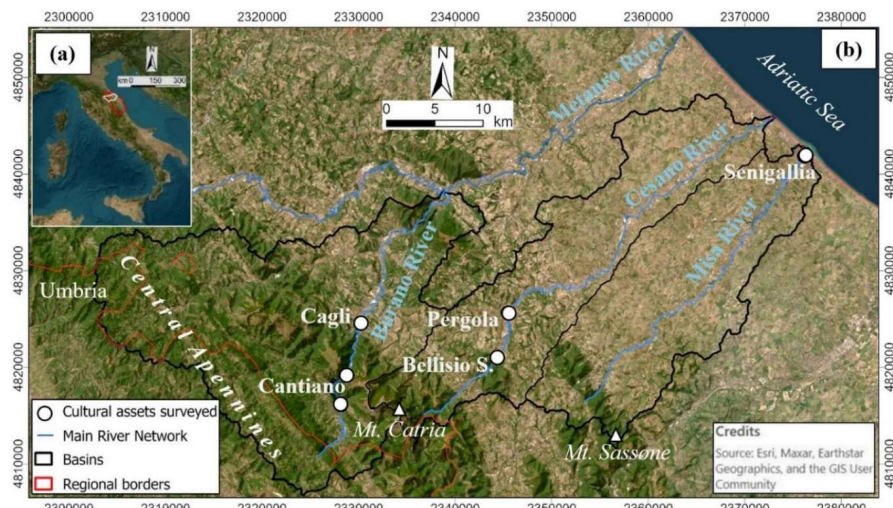
ha eliminato: Figure 1a,b

ha eliminato: Figure 1b

ha eliminato: Figure 1b

412 The CH assets damaged by the flood are included in the municipalities of Cantiano and Cagli (Burano basin), Pergola  
 413 and the hamlet of Bellisio Solfare (Cesano basin), and Senigallia (Misa basin), in Pesaro-Urbino and Ancona provinces.  
 414 These localities exhibit diverse historical and cultural attributes. The historical significance of Cantiano and Cagli is  
 415 notably linked to the ancient Roman road known as the "Flaminia," which was inaugurated between 223 and 202 B.C.  
 416 (Clini et al., 2023). One noteworthy site from the Roman period along the Via Flaminia is the Ponte Grosso bridge,  
 417 represented by the white dot between Cantiano and Cagli (Fig. 1b).

ha eliminato: Figure 1b



418  
 419 **Figure 1.** (a) The study area in Central Italy. In red is the border of the Marche Region, and in white is the area of the basins which  
 420 includes the assets involved during the flood that occurred on 15-16 September 2022. (b) The three basins that include the assets  
 421 affected by the flood: Burano, Cesano, and Misa. Coordinate system: WGS 1984 UTM Zone 33N.

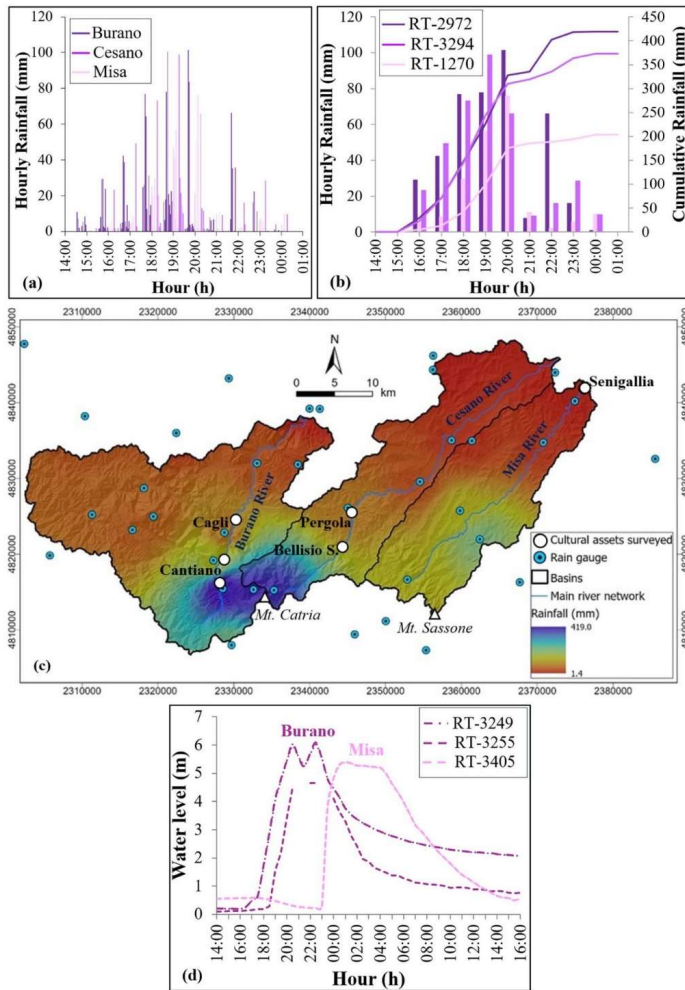
422 As for the Cesano basin, the site of Bellisio Solfare has a recent history starting from the late 1800s, with the beginning  
 423 of construction of the sulfur refinery. This location holds significance as part of the Marche Mining Geopark, established  
 424 in 2001 (Sulphur, MARCHE MINING GEOPARK, 2024). Pergola, known as the "city of hundred churches", has been  
 425 inhabited since Prehistory, with the cultural heritage most extensively documented originating from the Roman period.  
 426 The city of Senigallia has a rich historical background, as it was the first Roman colony to settle in the Adriatic coastal  
 427 plain. In the realm of flood risk management, the origins of protective measures can be traced back to the early Roman  
 428 settlements (De Donatis et al., 2019). Notably, the interventions were directed toward the construction of walls along the  
 429 course of the Misa River, with the dual function of both military and flood defense of the Senigallia city. The construction  
 430 of the walls, as well as other changes to the minor hydrographic network carried out by the Romans, preserved the city  
 431 from flooding by the Misa River. However, during the post-Roman age, the dismantling of these walls exposed a  
 432 significant portion of the city to floods, as evidenced by the event in 1472 and subsequent flooding between the 16th and  
 433 18th centuries A.D. The aftermath of these post-Roman age flood events, combined with continuous human interventions  
 434 contributed to shaping the current topography of the urban area in Senigallia (De Donatis et al., 2012).

### 435 3.2 The 15-16 September 2022 flood event

436 On 15-16 September 2022, following an extended period of drought in the preceding months (Pulvirenti et al., 2023), the  
 437 Northern Marche Region experienced very intense rainfall due to the formation of a stationary self-regenerating

439 thunderstorm system over the Apennine mountains, resulting in disastrous floods. From early afternoon on 15 September,  
 440 rainfall started to affect the Mt. Catria area, until it also extended to the mountainous areas of the Burano, Cesano, and  
 441 Misa basins. In Fig. 2 the rainfall and hydrometric data of the event are reported. The data were downloaded from the  
 442 Civil Protection monitoring system website of the Marche region (SIRMIP ON-LINE, 2024) and then elaborated.

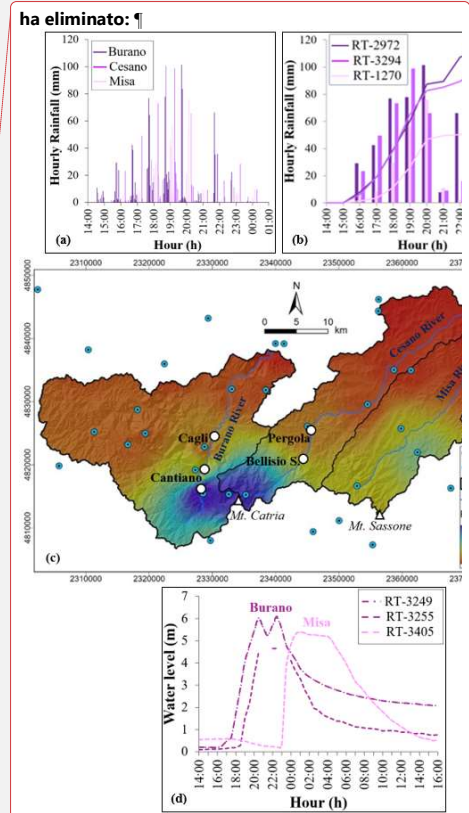
ha eliminato: Figure 2



443  
 444 **Figure 2.** Observed rainfall and flow rate of the 15-16 September 2022 event. a) Hourly rainfall measured by the rain gauges in the 3  
 445 basins; b) The 3 rain gauges\* of each basin that measured the maximum cumulative rainfall; c) Map of the cumulative rainfall; d)  
 446 Measured water level by hydrometer\*\* of the Burano River and Misa River. \*Rain gauges codes: “Cantiano RT-2972” (Burano basin);  
 447 “Monte Acuto RT-3294 (Cesano basin)”; “Colle RT-1270” (Misa basin). \*\*Hydrometers codes: “Pontedazzo RT-3249” (1 km  
 448 downstream Cantiano, Burano River) and “Cagli Ponte Cavour RT-3255” (Burano River); “Ponte Garibaldi RT-3405” (Senigallia,  
 449 Misa River). The shaded relief basemap of panel (c) was obtained from the TINITALY DEM (Tarquini et al., 2007, 2023). Distributed  
 450 under the CC BY 4.0 license. Coordinate system: WGS 1984 UTM Zone 33N.

451 The most intense phase of the event occurred between 18:00 and 19:00, with maximum hourly peaks of about 100 mm  
 452 recorded by stations near Mt. Catria, at the watershed between Burano and Cesano basins. In the Misa basin, the maximum  
 453 hourly peak was recorded at 19:30, amounting to about 80 mm (Fig. 2a, b).

ha eliminato: Figure 2a,b



458 The map of Fig. 2c, obtained interpolating the rain gauges data using the inverse distance weight interpolation method  
459 (Shepard, 1968) in ESRI™ ArcGIS Pro™ (IDW tool in Spatial Analyst Tools), highlights the high spatial variability of  
460 the rainfall event.

ha eliminato: Figure 2c

461 The rain gauges surrounding Mt. Catria, at the watershed between the Burano and Cesano basins, recorded the highest  
462 hourly rainfall intensity and cumulative rainfall, reaching 420 mm in 12 hours. In contrast, in the Misa basin, the maximum  
463 cumulative rainfall recorded northeast of Mt. Sassone is half the amount that has rained in the Mt. Catria area. In just 6  
464 hours, about half the precipitation that typically occurs on average in a year (i.e., 780 mm, REGIONE MARCHE,  
465 ANNALI IDROLOGICI, 2021) fell in the mountainous areas of the Burano, Cesano, and Misa basins. A return period of  
466 > 1000 years has been estimated for rainfall durations of 3-6-12-24 hours at the rain gauges located in areas characterized  
467 by higher rainfall intensities (REGIONE MARCHE, RAPPORTO DI EVENTO preliminare, 2022).

468 Although about half as much rain fell in the Misa basin as in the Burano and Cesano basins, the effects were still  
469 disastrous. One reason can be attributed to the different geology of the basins (e.g., Iacobucci et al., 2022). The Mt. Catria  
470 ridge in the Burano and Cesano basins mainly consists of fractured carbonate rocks, that contribute to the infiltration  
471 processes (Mastrorillo and Petitta, 2014), mitigating flood effects. On the other hand, the Misa basin is mainly composed  
472 of clays and sandstones, which are less permeable. As a result, a larger portion of the rainfall contributed to runoff  
473 processes, exacerbating flood dynamics.

474 The hydrometers reported in Fig. 2d, in the Burano basin, are located in the Pontedazzo section which is 1 km downstream  
475 from Cantiano (RT-3249), and in Cagli (RT-3255). The intense rainfall that fell over a brief period led to an abrupt  
476 increase in the river discharge, as highlighted by the water level variations of the Burano and Misa rivers (Fig. 2d). The  
477 blockage of bridges and culverted stretches significantly contributed to the flooding. In Cantiano, the flooding of the  
478 urban centre occurred from the culverted section of the Burano River, as shown in some videos recorded by residents  
479 (e.g., World Events News, 2022). In the case of Senigallia, a video shows the evolution of the flooding of the Misa River  
480 (Storm Chasers Marche, 2022). In this case, large woody debris crashed against the deck of the bridges "Corso 2 Giugno"  
481 and "Garibaldi" (where the hydrometer is located), causing widespread flooding throughout the city.

ha eliminato: Figure 2d

482 A total of 13 people died, and severe damage resulted in most settlements along the main rivers. Further details on flood  
483 dynamics in Cantiano, Cagli, Pergola, and Senigallia, and the consequent damage to CH assets, are provided in Sect. 4.2  
484 of the results.

ha eliminato: Figure 2d

## 485 4. Results and discussion

486 The results of applying the proposed method to assess the damage to CH assets caused by the flood event that occurred  
487 on 15-16 September 2022, in the Burano, Cesano, and Misa basins, are presented and discussed in two main sections.  
488 Sect. 4.1 concerns the analysis of the results obtained by applying the ex-post damage assessment method, which is the  
489 main goal of this paper. In Sect. 4.2 the results of the ex-ante application are compared with the ex-post results and then  
490 discussed. [The shapefile of the collected data and the ex-post damage assessment form are provided as supplementary](#)  
491 [materials to the paper \(see Data availability section\).](#)

### 492 4.1 Ex-post damage assessment

#### 493 4.1.1 Features of the CH assets and losses assessment



497 Remote analysis and field survey verification ensure the identification of all the CH assets actually damaged by the flood,  
 498 A total of 14 assets were identified, for which, maximum water level (MWL) baseline value (BV), and both losses in  
 499 intangible (LIV) and tangible (LTV) scores are provided in Table 4. Most of the damaged CH assets are religious building  
 500 types (6 out of 14), while the remaining damaged assets include bridges, a fortified gate, a square, a porch, and residential  
 501 or industrial architecture. Among the 14 assets identified, 3 of them (Ponte Garibaldi, S. Emidio oratory, and S. Maria del  
 502 Porto church) were not present in the MIC database and were therefore added as CH assets during the field survey,  
 503 according to the local authorities. Based on the suggestions of local authorities, even sites absent from the MIC database  
 504 should be considered of national significance, as they meet the criteria defined by national cultural heritage laws.  
 505 Therefore, the listing level for all 14 assets damaged by the 2022 Marche flood is classified as national.

506 Table 4 – CH assets damaged by the flood, classified by basin, type, MWL, and the associated scores of BV, LIV, and LTV.  
 507 Can: Cantiano; Cag: Cagli; P: Pergola; BS: Bellisio Solfare. All the assets in the Misa basin are located in Senigallia.

Basins	CH assets	Type	MWL (m)	BV (-)	LIV (-)	LTV (-)
Burano	(1) S. Emidio oratory (Cag)	Church	2.40	20	7	10
	(2) Ponte Grosso (Can)	Bridge	2.50	23	2.1	10
	(3) S. Agostino church (Can)	Church	0.35	27	0	5
	(4) S. Giovanni Battista collegiate (Can)	Church	1.40	27	13	15
	(5) S. Nicolò church (Can)	Church	2.05	24	5.1	10
	(6) Historical buildings Via Fiorucci (Can)	House	2.30	17	2.1	10
Cesano	(7) S. Maria delle Tinte church (P)	Church	3.40	37	20	15
	(8) Bellisio Solfare refinery (BS)	Factory	2.66	27	27	30
Misa	(9) Porta Lambertina	Fortified gate	0.44	17	0	5
	(10) S. Maria del Porto church	Church	0.06	21	0	5
	(11) Foro Annonario	Square	0.65	24	3	5
	(12) Portici Ercolani	Porch	1.50	17	0	5
	(13) Ponte Garibaldi	Bridge	2.18	6	6	15
	(14) Filanda Serica	Factory	0.23	10	0	5

508 Figure 3a shows the general view of the basins, and panels b-g highlight the distribution of the BV and LIV scores for the  
 509 sites of the three basins, while Fig. 4 reports the distribution of the LTV scores throughout the basins (panels b-g); panels  
 510 b1-g2 depicts two examples how the MWL was estimated during the field survey, in the case of a generic building and a  
 511 bridge, respectively; and in panels b1-c2 are reported two post-event photos showing the MWL. In the maps of Fig. 3 and  
 512 Fig. 4, the CH assets points correspond to the centroids of the polygon shapefile of the Marche regional cartographic data  
 513 portal (REGIONE MARCHE, Ambiente, 2023). In the cases of the S. Emidio oratory, and the two bridges Ponte Grosso  
 514 and Ponte Garibaldi, the polygonal shapefile of these assets was missing, hence their shape was digitized based on the  
 515 topographic map, and the centroid was extracted accordingly (as described in Sect. 2.2.4).

516 The most valuable cultural asset corresponds to the S. Maria delle Tinte Church (BV = 37), which is located in Pergola,  
 517 within the Cesano basin (Fig. 3, panel e7). The maximum aesthetic, historical, and communal values are assigned to that  
 518 asset, as the church was adorned with statues and stucco decorations, in addition to precious 18th-century wooden pews,  
 519 painted with floral motifs. Moreover, the church was built at the behest of the historical dyers and wool merchant guild,  
 520 and still today it is a representative place in the city. Indeed, after the 2022 flood, a committee called “Gli Angeli delle  
 521 Tinte” was assembled to propose a restoration project for the church (GLI ANGELI DELLE TINTE, 2024). In general,  
 522 religious architectures were built before the 19<sup>th</sup> century and, in addition to the high spiritual value, valuable structures  
 523 and valuable artworks coexist, resulting in a high aesthetic value. For these reasons, the average intangible value score of  
 524 the damaged churches is relatively high (BV = 26), in confront with the average score of the other asset types (BV =  
 525 18).

- ha eliminato: Through r
- ha eliminato: , the list of
- ha eliminato: was obtained
- ha eliminato: Table 4
- ha formattato: Tipo di carattere: 10 pt, Non Grassetto
- ha formattato: Tipo di carattere: 10 pt, Non Grassetto, Non Corsivo

- ha eliminato: Figure 3
- ha formattato: Tipo di carattere: 10 pt, Non Grassetto
- ha formattato: Tipo di carattere: 10 pt, Non Grassetto, Non Corsivo
- ha eliminato: Figure 4

- ha eliminato:
- ha eliminato: Figure 3

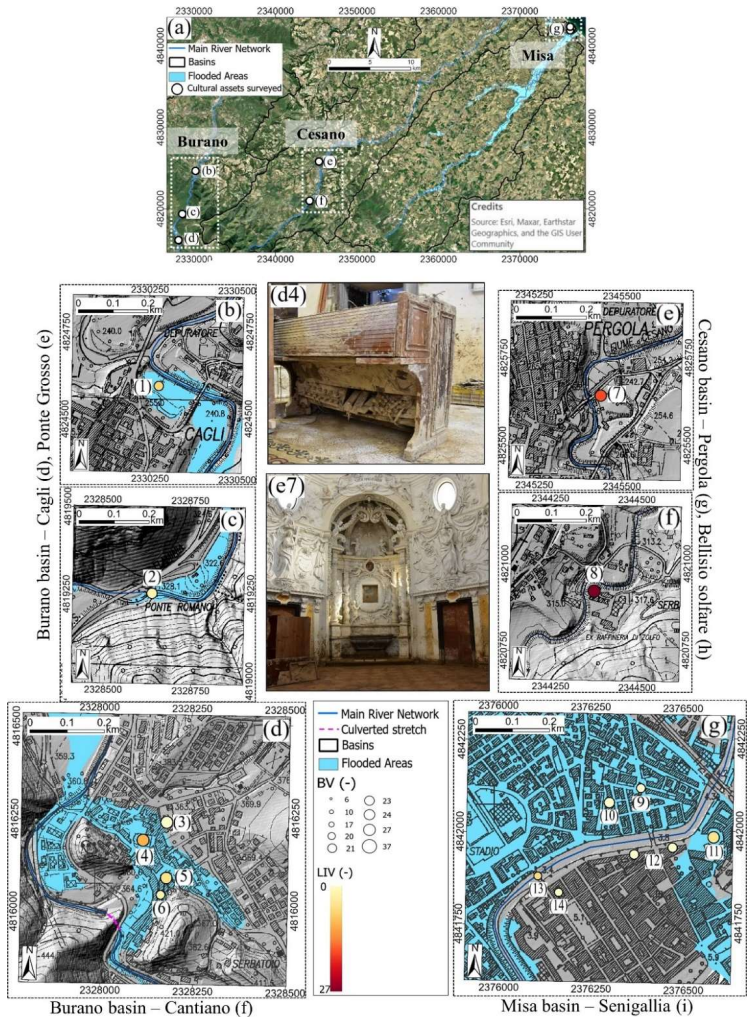
- ha eliminato: 19<sup>th</sup> century

535 Ponte Garibaldi (Fig. 3a, panel g13), namely the damaged bridge in Senigallia (Misa basin), has the lowest intangible  
 536 value ( $BV = 6$ ) for its limited historical value (it dates to the 1<sup>st</sup> mid of 20<sup>th</sup> century), as well as for its limited aesthetic  
 537 value. Indeed, even if it is an example of the typical early 20<sup>th</sup>-century architectural style, it is not a valuable structure.  
 538 On the other hand, the other damaged bridge in the Burano basin, Ponte Grosso in Cantiano (Fig. 3a, panel 3c), is  
 539 characterized by a higher intangible value ( $BV = 23$ ). In this case, even if its aesthetic value is limited, both the historical  
 540 and evidential values are high, because it is a rare example of infrastructure of the Ancient Rome Empire.

ha eliminato: Figure 3a

ha eliminato: 1<sup>st</sup> mid of

ha eliminato: Figure 3a



541  
 542 **Figure 3.** (a) General view of the CH assets surveyed for each basin; (b-g) the maps showing the  $BV$  (graduate symbols) and  $LIV$  (scale  
 543 colors) scores of the assets. Burano basin: (b) S. Emidio oratory in Cagli (1), (c) Ponte Grosso in Cantiano (2), and (d) the assets in  
 544 Cantiano (3-6); Cesano basin: (e) S. Maria delle Tinte Church (7), and (f) Bellisio Solfare (8); Misa basin: (g) the assets in Senigallia  
 545 (9-14). Panels d4 and e7 report post-event photos of S. Giovanni Battista collegiate and S. Maria delle Tinte church where damage as  
 546 a result of mud deposition inside the buildings is visible. The shaded relief basemap of panels (b-g) was obtained from the DTM LIDAR  
 547 of the Ministero dell'Ambiente e della Sicurezza Energetica (MASE, Geoportale Nazionale, 2024). The numerical technical map of  
 548 panels (b-g) is from the Marche Region (REGIONE MARCHE, Ambiente, 2023). Both maps are distributed under the CC BY 4.0  
 549 license. Coordinate system: WGS 1984 UTM Zone 33N.

Formattato: Mantieni con il successivo

ha eliminato: Fig. 1

554 It is worth noting that the Bellisio Solfare refinery asset (Fig. 3a, panel f8), despite being mostly unknown among the  
555 most important tourist attractions and with a poor state of conservation, is characterized by high intangible value ( $BV =$   
556 27). Indeed, it represented an important proof of the past industrial activity of the Pergola municipality area (Burano  
557 basin). Furthermore, a high communal value is assigned to it, due to the presence of an organization that aims to rebuild  
558 the asset.

ha eliminato: Figure 3a

559 The assets of Historical Buildings Via Fiorucci (Fig. 3a, panels d5) and Porta Lambertina (Fig. 3a, panel g9) are  
560 distinguished by their high historical significance, being notable architectures of the past, and holding a moderate aesthetic  
561 appeal, resulting in a  $BV = 17$ . In contrast, Foro Annonario (Fig. 3a, panel g11) and Portici Ercolani (Fig. 3a, panel g12),  
562 are CH open spaces of notable value, with  $BV = 24$ , and 17, respectively. While these two assets share similar evaluations  
563 across most value types, the Foro Annonario holds significant community value. Indeed, it represents the historical central  
564 marketplace of Senigallia, thus remaining a vital meeting point for the city since its realization.

ha eliminato: Figure 3a

ha eliminato: Figure 3a

ha eliminato: Figure 3a

ha eliminato: Figure 3a

565 Moreover, Fig. 3a (panels b-g) reports the extension of the flooded area from the Copernicus agency. In general, these  
566 maps agree with those actually flooded as a result of the event (the same for Fig. 4). The only exceptions are the areas of  
567 Pergola and Bellisio Solfare, as well as assets #12,14 in Senigallia. This demonstrates that these maps are useful for rapid  
568 identification of flooded areas. However, a direct field evaluation to establish which assets were effectively flooded is  
569 fundamental.

ha eliminato: Figure 3a

ha eliminato: Figure 4

570 In Fig. 4 are reported the maps showing the spatial distribution of the LTV scores of each asset (panels b-g). Concerning  
571 the Bellisio Solfare refinery (Fig. 4, panel f8), the highest LIV and LTV were assigned as the flood destroyed completely  
572 the building, and during the survey, only ruins were observed ( $LIV = 27$ , and  $LTV=30$ ). The historic S. Maria delle Tinte  
573 church (Fig. 4, panel e7) sustained considerable damage caused by the flood, both in terms of damage to intangible and  
574 tangible value ( $LIV = 20$ , and  $LTV=15$ ). The inundation resulted in harm to the electricity system and the emergence of  
575 mold on both the floor and wall paintings. Additionally, the force of the floodwater partially wrecked the door and  
576 destroyed the 18th-century pews. As a result, the aesthetic value of the church was deemed lost. Moreover, its extended  
577 closure period led to a significant impact on its communal value. Even the S. Giovanni Battista collegiate (Fig. 4, panel  
578 3f) experienced severe damage ( $LIV = 13$ , and  $LTV=15$ ). In addition to the effects already observed for the other assets,  
579 floor tiles were broken, the wooden choir and altars were swollen due to the floodwater, and the 16th-century liturgical  
580 supply was covered by mud. In the case of S. Nicolò church (Fig. 4, panel d5), part of the floor collapsed, and the external  
581 stone and metal balustrade were swept away by the flowing water ( $LIV = 5.1$ , and  $LTV=10$ ). Similar loss scores were  
582 observed for the St. Emidio oratory (Fig. 4, panel b1), in which, however, a significant loss was due to the wooden door  
583 as it was swept away.

ha eliminato: Figure 4

ha eliminato: Figure 4

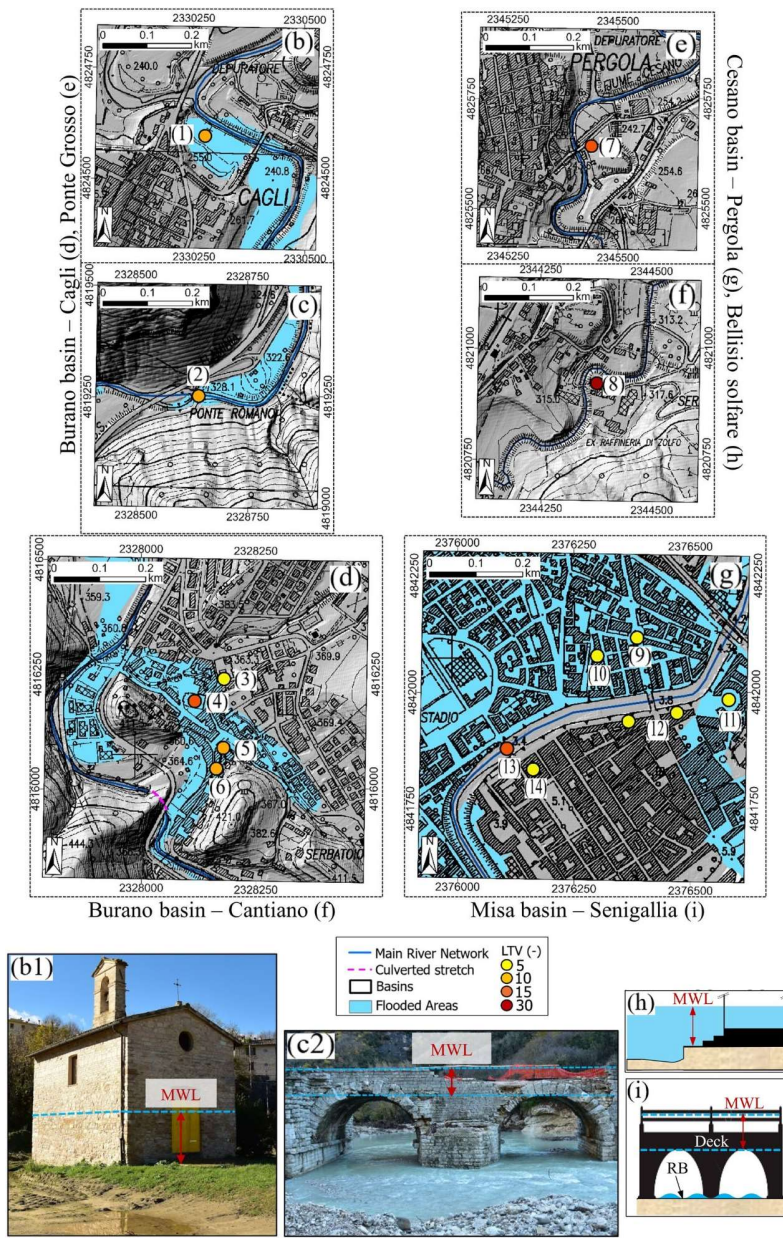
ha eliminato: Figure 4

ha eliminato: Figure 4

ha eliminato: Figure 4

ha eliminato: Figure 4





597

598 **Figure 4.** (d-i) The maps of the LTV scores of the assets. Panels (b1) and (c2) display the post-event field survey photos depicting the  
 599 damage to the S. Emidio oratory and Ponte Grosso, respectively. Panels (h) and (i) report the schematic view of the MWL estimation  
 600 in the case of a generic building and a bridge, respectively. (RP is the reference point used for the measurement of the MWL, and RB  
 601 is the riverbed). The shaded relief basemap of panels (b-g) was obtained from the DTM LIDAR of the Ministero dell'Ambiente e della  
 602 Sicurezza Energetica (MASE, Geoportale Nazionale, 2024). The numerical technical map of panels (b-g) is from the Marche Region  
 603 (REGIONE MARCHE, Ambiente, 2023). Both maps are distributed under the CC BY 4.0 license. Coordinate system: WGS 1984  
 604 UTM Zone 33N.

605 Overall, a high level of losses was observed for most of the affected religious structures, where closure due to extensive  
606 damage contributed to a decrease in communal value. Conversely, the S. Agostino (Fig. 4, panel d3), and Porta  
607 Lambertina, S. Maria del Porto, Portici Ercolani, and Filanda Serica assets (Fig. 4, panels g9,10,12, and 14) incurred the  
608 lowest losses, both in intangible and tangible aspects  $LIV = 0$ , and  $LTV=5$ . Specifically, the two churches were not  
609 damaged as they are over-elevated from the ground floor. For all these assets, only mud marks dirtied the external walls.  
610 As regards the Foro Annonario (Fig. 4, panel g11), the only damage is related to the mud marks along the porch perimeter.  
611 Nevertheless, the relative  $LIV$  is higher than 0 ( $LIV = 3$ ) since the circular square in which the porches are located  
612 remained impracticable for some days.

613 The two affected bridges were significantly damaged as the maximum level reached by the water during the flood  
614 exceeded the height of the deck. Portions of the arch stones of the Ponte Grosso (Fig. 4, panel c2) collapsed leading to a  
615 moderate decrease in tangible value ( $LTV=10$ ). However, the historical and evidential aspects remained unscathed,  
616 resulting in a relatively low decline in intangible value ( $LIV = 2.1$ ). Conversely, the Ponte Garibaldi (Fig. 4, panel g13)  
617 sustained severe structural damage ( $LTV=15$ ). Indeed, some months after the field survey, it ultimately had to be  
618 demolished (ANSA, Regione Marche, 2023), resulting in the loss of aesthetic and historical significance ( $LIV = 6$ ).

619 Regarding the MWL estimate (Fig. 4, panels h,i), it was directly measured during the field survey, as detailed in Sect.  
620 2.2.2. However, there were exceptions with the two bridges and the Bellisio Solfare refinery. Direct measurements were  
621 not possible in these instances due to the inaccessibility of the bridges, compounded by the destruction of the Bellisio  
622 Solfare asset. Consequently, for these cases, the estimation of MWL was conducted indirectly. As for the Ponte Grosso  
623 (Fig. 4, panel c2), the MWL was estimated considering wood deposition height at road signals close to the bridge (e.g.,  
624 video from TGC0M24, 2022). The resulting estimated MWL from the deck is 2.5 m. With regards to Ponte Garibaldi  
625 (Fig. 4, panel g13), the highest water level value from the riverbed was recorded during the flood peak by the hydrometer  
626 on the Misa River (i.e., 5.39 m as reported in Fig. 2d). The height from the riverbed to the base of the deck was estimated,  
627 and this value was subtracted from the maximum height measured by the hydrometer, resulting in a MWL of 2.18 meters.

628 In the case of the Bellisio Solfare asset (Fig. 4, panel f8), the MWL was estimated by considering the mud marks height  
629 at the closest building on the hydrographic left of the Cesano River. The measured MWL at this building, used as a  
630 reference, is 1.45 m. Thus, considering the DTM difference between the refinery and this site, the resulting MWL at  
631 Bellisio Solfare is equal to 2.66 m.

632 Moreover, as the cultural assets listed in Table 4 are mostly located on flat areas, the measured  $Aq$ , as defined in Sect.  
633 2.2.2, is negligible.

#### 634 4.1.2 Factors influencing flood damage

635 In this study, the following factors were considered as those that can potentially contribute to the damage to CH assets:  
636 maximum water level outside the construction (MWL), maximum water level inside the construction ( $mwl$ ), minimum  
637 distance between asset and river ( $\Delta D$ ), difference between the elevation of CH asset and the elevation of the riverbed  
638 ( $\Delta E$ ); difference between DTM and filled DTM ( $\Delta DTM$ ), average slope of the river (RS), local slope (LS), curvature  
639 (CU), Topographic Wetness Index (TWI), Terrain Ruggedness Index (TRI).

640 The procedures described in Sect. 2.2.2 allowed us to investigate which factors contributed significantly to both the  $LTV$   
641 and  $LIV$  of the CH assets. Considering the  $mwl$  and  $hg$  parameters, as they were only available for a few assets, it were  
642 not included in the damage inference analysis. Among all the factors analyzed, RS, MWL, and  $\Delta E$  showed some  
643 correlation to  $LTV$  (Fig. 5a-c), while for all others contributing factors the correlation proved to be negligible. The same

ha eliminato: Figure 4

ha eliminato: Figure 4

ha eliminato: Figure 4

ha eliminato: Figure 4

ha eliminato: Figure 4

ha eliminato: Figure 4

ha eliminato: Figure 4

ha eliminato: Figure 4

ha eliminato: Figure 2d

ha eliminato: Figure 4

ha eliminato: Table 4

ha formattato: Tipo di carattere: 10 pt, Non Grassetto

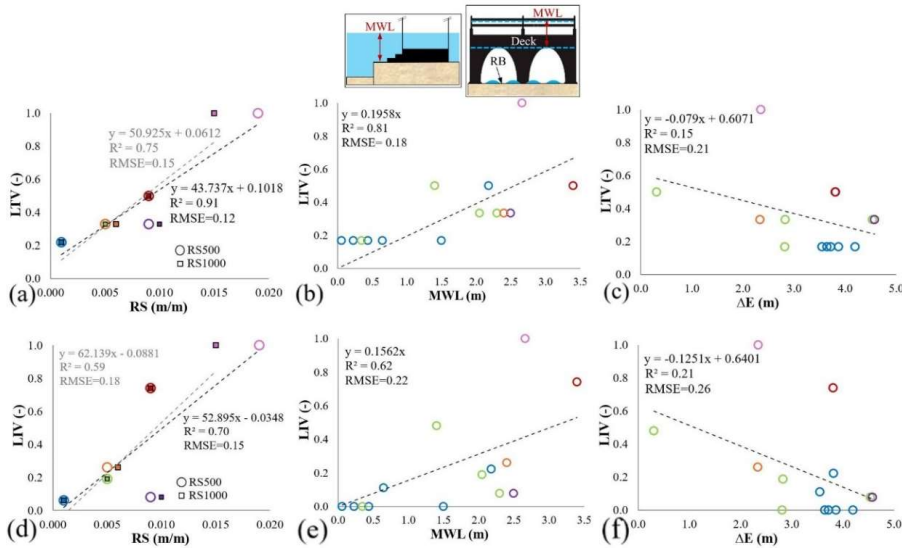
ha formattato: Tipo di carattere: 10 pt, Non Grassetto,  
Non Corsivo

ha eliminato: Figure 5a-c

ha eliminato:

657 trend resulted also correlating the *LIV* with the same contributing factors (Fig. 5d-e). This can be explained as the *LIV* is  
 658 linked to the LTV. Indeed, if an asset is destroyed, all the intangible values are lost too. Overall, there is a greater  
 659 correlation between LTV and contributing factors than *LIV*, as the aspects that are not strictly related to physical  
 660 parameters are considered when assessing *LIV*.

ha eliminato: Figure 5



661  
 662 **Figure 5.** Relations between normalized LTV (a-c) and *LIV* (d-e) with influencing contributing factors: (a,d) RS, considering distances  
 663 of 500 m (black line and circles) and 1000 m (grey line and boxes) upstream from the single asset or group of assets; (b,e) MWL  
 664 measured as the height of the maximum water/mud mark level with respect to the outside ground floor of each asset; (c,f)  $\Delta E$ , the  
 665 elevation difference between the asset and the riverbed.

666 The factors RS and LTV (Fig. 5a), considering the 500 m stretch upstream of the single asset of a group of assets (RS500),  
 667 exhibit both a higher correlation and a lower dispersion ( $R^2=0.91$ ,  $RMSE=0.12$ ). Also considering the 1000 m stretch  
 668 upstream from the CH (RS1000), the LTV-RS relationship is clear, although it results in a lower correlation and greater  
 669 dispersion ( $R^2=0.75$ ,  $RMSE=0.15$ ) than considering the RS500 factor. These results show that an increase in RS  
 670 corresponds to an increase in LTV. Both 500 m and 1000 m were considered as there are no clear recommendations in  
 671 the literature on whether the flow of a river adapts to the slope of the riverbed. Nevertheless, considering these distances,  
 672 it is reasonable to assume that the slope of the riverbed affects the energy of the flowing water and thus can be used as a  
 673 valid proxy for current velocity. As observed, the dynamics of the flood event were different throughout the basins (Sect.  
 674 3.2). In the case of the Misa River in Senigallia (RS500,1000=0.001 m/m), the flooding that occurred was mainly caused  
 675 by the overtopping of the 2 bridges present, which in turn caused a progressive and slow rise in water levels throughout  
 676 the city. This scenario resulted in damage to CH primarily attributable to water stagnation and the accumulation of fine  
 677 sediments (ranging from clays to sands), rather than the direct impact of hydrodynamic forces from flowing water. Indeed,  
 678 for all the CH assets, the minimum LTV (5) was observed (Table 4). The only exception is the Garibaldi Bridge, which  
 679 was more severely damaged ( $LTV=15$ ) as it was obstructed due to the passage of woody debris and the related pressure  
 680 exerted on it. On the other hand, for the sites in the Burano and Cesano basins, a steeper slope caused greater damage due  
 681 to the hydrodynamic force of the water impacting the CH assets. This is evidenced by some videos recorded at Cantiano  
 682 (as described in Sect. 3.2), but especially by the destruction of the Bellisio Solfare refinery ( $LTV=30$ ). In this case, the

ha eliminato: Figure 5a

ha eliminato: Table 4

ha formattato: Tipo di carattere: 10 pt, Non Grassetto

ha formattato: Tipo di carattere: 10 pt, Non Grassetto, Non Corsivo

686 slope of the Cesano River was sufficient to transport and deposit large amounts of floating and coarse debris, including  
687 wood, gravel, and boulders, which contributed to the destruction of the site. However, it is also worth noting that this site  
688 was in a poor state of conservation, that possibly reduced structural resistance.

689 As concerns the correlation between LTV and MWL, Fig. 5b highlights a clear relationship. Namely, the higher the flood  
690 depth, the greater the damage, as generally found in the literature for stage-damage functions. However, a lower  
691 correlation is observed than the LTV-RS500 relationship as well as also a higher dispersion ( $R^2=0.81$ ,  $RMSE=0.18$ ). A  
692 higher RMSE value can be justified by the Bellisio Solfare site, which represents an outlier. Indeed, the maximum  
693 assigned LTV value due to its destruction is not solely linked to the MWL, but rather to the energy of the flow, as  
694 demonstrated above. The lowest correlation and the highest dispersion ( $R^2=0.15$ ,  $RMSE=0.21$ ) correspond to the LTV-  
695  $\Delta E$  relationship (Fig. 5c).

ha eliminato: Figure 5b

696 Overall, the following results are worth highlighting:

- 697 • The correlation between LTV and *LIV* with  $\Delta E$  is not statistically significant ( $p\text{-value} > 0.05$ ).
- 698 • LTV and *LIV* are highly correlated (Pearson's  $R=0.93$  and  $p\text{-value} < 0.05$ ). Despite *LIV* considering factors not  
699 directly related to the physical characteristics of a flood event, it still correlates well with LTV. Indeed, aesthetic  
700 and communal value losses are generally sensitive to flood impacts, while evidential and historical values persist  
701 despite flood damage, as the asset remains a testament to historical eras and past activities. However, if the asset  
702 is destroyed, also intangible values are lost.
- 703 • RS (i.e., a proxy for river flow velocity) is highly correlated with LTV and *LIV* (Pearson's  $R=0.85$  and  $0.84$ ,  
704 respectively, and  $p\text{-value} < 0.05$ ) but not significantly correlated with MWL (Pearson's  $R=0.62$  and  $p\text{-value} >$   
705  $0.05$ ). Therefore, both RS and MWL are crucial for accurately estimating damage.

ha eliminato: Figure 5c

706 The obtained results derive from specific criteria for assigning LTV and *LIV* scores, which rely on an expert-judgment-  
707 based quantification method. Therefore, a discussion of how correlations change considering different scores of LTV and  
708 *LIV* is needed. To achieve this, the analysis is conducted using scores that vary both linearly and nonlinearly, categorized  
709 into four classes to ensure comparability with the approach used in this paper. Concerning the LTV, using a linear scale  
710 (LTV=5-10-15-20), the relations obtained are very similar to those resulting from the scale used in this paper. Although  
711 small variations in  $R^2$  and RMSE occur, the trends obtained are practically the same, with high correlation with RS500  
712 and RS1000 and very low correlation with  $\Delta E$ . The largest differences occur in the case of MWL, with a significant  
713 increase in the correlation ( $R^2=0.88$ ). Even using a fully non-linear scale (LTV=5-10-20-40), the general trend remains  
714 the same, with an increase in the correlation with MWL ( $R^2=0.75$ ) compared those obtained with the scale adopted in this  
715 paper. Regarding the *LIV*, we changed the score of *V*, again varying it linearly and non-linearly, and using maximum and  
716 minimum values the same as proposed in Romão and Paupério (2021). In the case of linear ( $V =0-6.7-13.3-20$ ) and non-  
717 linear ( $V =0-3-12.5-20$ ) variation, the trend is the same with those obtained in this paper, with a slightly worse correlation  
718 using a non-linear scale. Overall, varying linearly and nonlinearly the scores of LTV and *LIV* results in trends consistent  
719 with those observed using the scales adopted in this paper. This supports the conclusion that there is a significant  
720 relationship between tangible and intangible damages and the contributing factors analysed.

721 As mentioned in Sect. 2.2.4, also intrinsic factors can potentially influence the damages to CH. In this regard, a relevant  
722 aspect to consider when measuring the maximum water level inside the building (*mwl*) and assessing the vulnerability of  
723 a CH asset, but in general of any building, is the possible presence of basements. Typically, basements increase the  
724 vulnerability of a structure to flooding, as they can lead to a higher *mwl*. However, it is not always the case that a higher  
725 *mwl* is reached at the basement level than at the upper floors. Indeed, this depends on how and whether the basement  
726 floors are hydraulically connected to the upper floors or the outside of the building. However, if the presence of the

729 basement results in a higher water level in the basement, but a lower water level on the ground floor, this could potentially  
730 reduce the observed losses. In this scenario, if the movable artworks are mostly exposed at the ground level, they may  
731 remain unaffected by the floodwater. In general, for a CH asset with several flooded floors, including the basement, it  
732 may be appropriate to measure the mwl and evaluate LTV and LIV on each floor. Then, the related average values for  
733 the entire asset can be considered for further analysis.

734 Moreover, also the presence of valuable contents, especially if exposed at a low level with respect to the ground floor,  
735 increases the amount of damage, and then the restoration cost. Indeed, the religious architectures that contain paintings,  
736 precious pews, and ancient elements such as organs, have incurred in moderate or severe LTV, specifically the churches  
737 of S. Maria delle Tinte, S. Giovanni Battista, and S. Nicolò (Table 4). On the other hand, although the S. Agostino and S.  
738 Maria del Porto churches contain artworks, they have not experienced a loss in tangible value. This is attributed to their  
739 elevated positioning above ground floor level. However, it could be noteworthy that their low LTV can also be attributed  
740 to their relatively low MWL (Table 4). A more explanatory perspective on the positive impact of elevation on damage is  
741 the S. Nicolò church. Indeed, in this case, despite a high MWL, the associated LTV is relatively low, as it is supra-elevated  
742 at 1.12 m above ground floor level (Table 4).

743 Even the state of conservation could influence the degree of damage. Indeed, the poor state of conservation reduced the  
744 Bellisio Solfare asset capacity to resist the impact of the water and debris mixture, contributing to its destruction. This  
745 data confirms that the degree of conservation can directly impact the extent of damage observed following a flood event  
746 (Stephenson and D'Ayala, 2014; Salazar et al., 2024).

747 Studies in literature pinpoint the role of construction material in determining the vulnerability of CH assets (Balasbaneh  
748 et al., 2020; Brokerhof et al., 2023). However, no relations were found for this parameter, as all the surveyed assets are  
749 characterized by the same material (i.e., masonry structure). The only exception is the Ponte Garibaldi, which was  
750 constructed with a reinforced concrete structure.

751 Among the factors that have contributed significantly to the overflowing of rivers during the 2022 Marche flood event  
752 are bridges and culverts, which were clogged. In Cantiano, the inadequacy of the culverted section at the entrance of the  
753 urban area resulted in insufficient drainage of the Burano River, leading to overflow and sediment deposition. In Pergola,  
754 a bridge near the S. Maria delle Tinte church was blocked by sediment and woody debris, resulting in flooding of the  
755 surrounding area. In Senigallia, large woody debris blocked Ponte Garibaldi, causing the flooding of the city. It is widely  
756 observed that bridges and culverts can become clogged during intense bed load transport, hyper-concentrated flow, or  
757 debris flow events, leading to massive overflows. To mitigate the risk of clogging in complex urban environments, a river  
758 management approach that incorporates optimized design principles based on adequate field surveys, numerical  
759 modelling, and laboratory experiments is desirable (Gschntzer et al., 2017; Amaddii et al., 2022, 2023; Martín-Vide et  
760 al., 2023; Zugliani et al., 2023). These measures would also positively impact the preservation of ancient CH assets, which  
761 are now confronted with heightened flood risks due to climate change, a risk likely lower during their construction.

#### 762 4.2 Comparison between ex-post and ex-ante damage assessment

763 In this section, the results obtained through the methodology outlined in Sect. 2.1 are presented and compared to the  
764 results of the ex-post damage assessment, considering only the LTV.

765 The first issue with the flood hazard map is its low degree of detail. Indeed, all the areas investigated are in the same  
766 class, namely “medium probability (low-frequency floods)”, and the map lacks some useful information, such as water  
767 height or velocity. Thus, assets can only be included or excluded from floodable areas. Overlapping the assets of the MIC

ha eliminato: Table 4

ha formattato: Tipo di carattere: 10 pt, Non Grassetto

ha formattato: Tipo di carattere: 10 pt, Non Grassetto,  
Non Corsivo

ha eliminato: Table 4

ha formattato: Tipo di carattere: 10 pt, Non Grassetto

ha formattato: Tipo di carattere: 10 pt, Non Grassetto,  
Non Corsivo

ha eliminato: Table 4

ha formattato: Tipo di carattere: 10 pt, Non Grassetto

ha formattato: Tipo di carattere: 10 pt, Non Grassetto,  
Non Corsivo



771 database with the official map of flood hazard areas, 55 potentially damaged assets were identified. These assets were  
 772 then categorized based on their typology into various damage classes: 41 are included at risk of very high damage, 6 as  
 773 high, 5 as medium, and 2 as low. One of the individuated assets (“Fiorentino Basso”) remains unclassified due to  
 774 insufficient information available in the MIC database regarding its type. Additionally, the MIC database lacks  
 775 information regarding the type of value associated with each asset. It is noteworthy that only 5 in 55 identified assets are  
 776 listed as damaged cultural heritage (Ponte Grosso, S. Giovanni Battista collegiate, S. Maria delle Tinte church, Porta  
 777 Lambertina, and Foro Annonario in Table 4), based on the definition of cultural heritage given in section 2.2.1. Indeed,  
 778 38 assets are residential, productive, rural, tertiary architectures, or open space that do not reflect the cultural heritage  
 779 definition mentioned in Sect. 2.2.1. Consequently, no data were collected for them, and it is unknown whether they were  
 780 affected by the flood. Moreover, 11 of the 55 assets are religious architectures, historical infrastructures, and open spaces  
 781 with cultural interest (as defined in Sect. 2.2.1). Although these assets are located in flood hazard areas, they were not  
 782 actually damaged by the flood and thus were not considered in this paper.

783 In addition, it should be emphasized that 9 assets defy the ex-ante damage assessment, even if identified as damaged  
 784 during the field survey. This discrepancy arises either from their absence in the MIC database (such as Ponte Garibaldi,  
 785 S. Emidio oratory, and S. Maria del Porto church) or because they do not overlap with the flood hazard areas (including  
 786 Portici Ercolani, Bellisio Solfare refinery, Filanda Serica, historical buildings Via Fiorucci, S. Agostino church, and S.  
 787 Nicolò church).

788 These findings highlight the main issues with the MIC database:

- 789 • Some assets may be inaccurately geo-localized (e.g., Bellisio Solfare refinery).
- 790 • In cases where assets have an extended area and only a small portion is potentially inundated, the point shapefile  
 791 may not accurately represent their exposure, as it could be situated in unexposed areas (as observed with the  
 792 historical buildings Via Fiorucci and S. Agostino church). In the case of widespread assets or constructions with  
 793 a linear footprint (i.e., assets including several buildings along a road, or porches such as Portici Ercolani) only  
 794 one centroid point representative of the location exists.

795 Consequently, the comparison between the ex-ante and the ex-post damage assessments is feasible only for five assets:  
 796 Porta Lambertina, Ponte Grosso, Foro Annonario, S. Giovanni Collegiate, and S. Maria delle Tinte church. Consistently  
 797 with observations, from the ex-ante damage assessment it derives that the two churches fall in a very high damage class,  
 798 the Ponte Grosso bridge falls in a medium damage class, and the open space Foro Annonario falls in a low damage  
 799 class. Observed losses thus confirm that religious architectures are the most vulnerable to flooding as assumed in most of  
 800 the ex-ante flood risk assessment works in literature (Garrote et al., 2020; Arrighi et al., 2023). Concerning Porta  
 801 Lambertina, it resulted in a high damage class, while the ex-post assessment resulted in being slightly damaged, as only  
 802 mud marks were observed.

### 803 5. Conclusions

804 This paper developed an ex-post flood damage assessment method for CH assets. This yields a semi-quantitative on-site  
 805 evaluation of losses (i.e., not in monetary terms), both in terms of intangible and tangible impacts, that based on the best  
 806 of our knowledge constitutes a novel aspect. The method consists of four main steps: (i) identifying CH assets potentially  
 807 damaged by the flood; (ii) collecting post-event field data, through an ad-hoc developed survey form; (iii) evaluating the  
 808 losses in both intangible and tangible values; and (iv) analyzing the factors contributing to flood damage. For step (ii), it  
 809 is crucial to visit the damaged sites as soon as possible to collect data and information that may become unavailable due

ha eliminato: Table 4

ha formattato: Tipo di carattere: 10 pt, Non Grassetto

ha formattato: Tipo di carattere: 10 pt, Non Grassetto, Non Corsivo

ha eliminato: 37

ha eliminato: cultural

ha eliminato: or

ha eliminato: with no local or touristic/cultural interest

ha eliminato: some

ha eliminato: or

ha eliminato: that

ha eliminato: were not

ha eliminato: during the 15-16 September 2022 event.

Formattato: SpazioDopo: 0 pt

ha eliminato: ted

Formattato: SpazioDopo: 0 pt

821 to restoration work. The use of the proposed form allows a quick easy, and reproducible way for the post-event flood data  
822 evaluation aimed at the direct assessment of losses in intangible and tangible values to CH assets. Then, step (iii) allows  
823 us to estimate the level of losses caused by floods on both tangible and intangible values to different types of CH assets.  
824 Finally, the findings from step (iv) allow for a better understanding of the causative phenomena aimed at valuable insights  
825 for disaster risk management.

826 The method was applied to the CH assets damaged by the flood event that occurred on September 15-16 in the Burano,  
827 Cesano, and Misa basins (Marche Region, Italy). The main findings that can be drawn from the application of the proposed  
828 method are the following:

- 829 • Post-event field survey is fundamental for gathering data and information on the hazard characteristics, such as  
830 water depths, together with losses in intangible and tangible values and for subsequent analysis (e.g., GIS  
831 processing). Ex-post flood damage information for CH is relevant for verifying the hypothesis of existing  
832 methods based on expert judgement. Moreover, it poses the basis for developing empirical flood vulnerability  
833 functions for CH. Peculiarities of CH, such as raised floors, presence of valuable artworks, and state of  
834 conservation are found to be relevant for flood vulnerability. Thus, where this information is not available, on-  
835 site inspections are suggested to better characterize actual exposure and vulnerability for ex-ante risk analysis.
- 836 • The LTV is well correlated with the MWL, consistently with damages to other constructions types. Additionally,  
837 there is also a strong correlation between LTV and the average slope of the riverbed, considering both 500 m  
838 and 1000 m upstream of the assets. The slope of the riverbed, a proxy of river flow velocity, can thus be  
839 considered as one of the possible contributing damage factors (as the measured or estimated data of water  
840 velocity is difficult to obtain).
- 841 • The *LIV* correlates well to the same contributing factors, however, *LIV* data show a lower  $R^2$  and a larger spread  
842 demonstrating that intangible aspects are less dependent on flood characteristics. Nevertheless, LTV and *LIV*  
843 are highly correlated, since some intangible values, e.g., aesthetic and communal values are sensitive to physical  
844 flood damage, e.g., lack of accessibility.
- 845 • RS (i.e., a proxy for river flow velocity) is highly correlated with LTV and *LIV* but not significantly correlated  
846 with MWL, and therefore, both RS and MWL are crucial for accurately estimating damage.
- 847 • The robustness of these correlations is further enhanced as testing different scales, whether varying linearly or  
848 nonlinearly, yields the same results.

849 However, the method also presents some limitations:

- 850 • The baseline pre-disaster intangible value is obtained by combining four different typologies of value (aesthetic,  
851 historical, evidential, communal) making some assumptions to identify the criteria for assigning the level of  
852 value to each intangible aspect. Additional or alternative aspects, not currently accounted for, could influence  
853 the assignment of intangible value.
- 854 • The limited number of surveyed assets does not allow for statistically robust relationships with contributing  
855 factors. Indeed, other potential contributing factors could affect the observed damage (e.g., construction  
856 material).

857 The existing exposure and vulnerability models, such as those by Arrighi et al. (2023), provide reasonable initial  
858 predictions of potential damage to cultural heritage (CH). However, it should be emphasized that the available exposure  
859 data are incomplete and inadequate for identifying all the flood-exposed assets and their vulnerability, leading to  
860 inaccurate ex-ante damage assessments to CH, specifically:

ha eliminato: building

- 862
- In the Burano, Cesano, and Misa basins, the official flood hazard map lacks the necessary detail to distinguish which assets may suffer low or high flood damage, as it does not provide information on flood magnitude, such as water depth and velocity.
- 863
- The MIC database includes immovable and movable assets encompassing those currently under protection, and also those under verification. Therefore, an on-site direct check, conducted in collaboration with local authorities, is always necessary to determine whether an asset qualifies as cultural heritage. Furthermore, the database does not offer any information to delineate the value of assets, and in some cases, they are not accurately geo-localized.
- 864
- 865
- 866
- 867
- 868
- 869

870 This paper underscores the importance of post-flood data collection and analysis. The proposed method serves as a starting point for such data collection. Nevertheless, future research should include diverse cultural and geographic contexts to improve accuracy, as the contributing factors can differently influence the observed damage. An open-source, comprehensive CH database documenting flood-related damages, asset features (e.g., construction type, and construction material), and factors describing the event magnitude (e.g., maximum water level) is needed. Additionally, quantifying tangible damage in monetary terms should allow us to obtain a more robust evaluation of the damage to CH assets. Nonetheless, it requires collaboration with government institutions to share monetary data (e.g., restoration costs). These steps would enhance flood risk management for CH conservation and help develop robust damage prediction models.

871

872

873

874

875

876

877

ha eliminato: building

878 *Data availability.* GIS data and ex-post damage survey form will be made available in a public repository after acceptance.

879 *Author contributions.* CA conceptualized the research idea; CA and CDL equally contributed to the planning of the on-site data collection and performed the measurements; CA, CDL, and MA developed the methodology; MA, CDL, and CA analyzed the data; MA performed GIS analysis; MA handled the data visualization; CA supervised the research activity; MA and CDL wrote the manuscript draft; CA reviewed and edited the manuscript.

880

881

882

883 *Competing interests.* The authors declare that they have no conflict of interest.

884 *Acknowledgements.* The authors express their gratitude to the working group “MARCHE 2022” (<https://sites.google.com/view/misa2022/home-page>) for their collaboration in the post-event data collection phase. [A sincere acknowledgment goes to the technical offices of the municipalities of Senigallia, Cantiano, Pergola and Cagli and to Don M. Cardoni for their support.](#)

885

886

887

888 *Financial support.* This study was carried out within the RETURN Extended Partnership and received funding from the European Union Next-Generation EU (National Recovery and Resilience Plan – NRRP, Mission 4, Component 2, Investment 1.3 – D.D. 1243 2/8/2022, PE0000005).

889

890

## 891 **References**

892 [Adeyemo, O.J., Maksimovic, C., Booyan –Aaronnet, S., Leitao, J., Butler, D., and Makropoulos, C.: Sensitivity analysis of surface runoff generation for Pluvial Urban Flooding, in: 11th International Conference on Urban Drainage, Edinburgh, Scotland, UK, <https://api.semanticscholar.org/CorpusID:128436486>, 2008.](#)

893

894 [Al-Kindi, K.M. and Alabri, Z.: Investigating the role of the key conditioning factors in flood susceptibility mapping through machine learning approaches, \*Earth Syst Environ\* 8, 63–81, <https://doi.org/10.1007/s41748-023-00369-7>, 2024.](#)

895

896



928 [Alexandrakis, G., Manasakis, C., and Kampanis, N.A.: Economic and societal impacts on cultural heritage sites, resulting](#)  
929 [from natural effects and climate change. \*Heritage\*, 2, 279-305, <https://doi.org/10.3390/heritage2010019>, 2019.](#)

930 [Amaddii, M., Rosatti, G., Zugliani, D., Marzini, L., and Disperati, L.: Back-analysis of the Abbadia San Salvatore \(Mt.](#)  
931 [Amiata, Italy\) debris flow of 27–28 July 2019: an integrated multidisciplinary approach to a challenging case study,](#)  
932 [Geosciences, 12, 385, <https://doi.org/10.3390/geosciences12100385>, 2022.](#)

933 [Amaddii M., Rosatti G., Zugliani D., Marzini L., and Disperati L.: Modelling stony debris flows involving culverted](#)  
934 [streams: the Abbadia San Salvatore case \(Mt. Amiata, Italy\), \*Rend. Online Soc. Geol.It.\*, 61, 108-115,](#)  
935 [https://doi.org/10.3301/ROL.2023.55, 2023.](#)

936 [Anderson, K.: The impact of increased flooding caused by climate change on heritage in England and North Wales, and](#)  
937 [possible preventative measures: what could/should be done?, \*Built Heritage\* 7, 7, \[https://doi.org/10.1186/s43238-023-\]\(https://doi.org/10.1186/s43238-023-00087-z\)](#)  
938 [00087-z, 02, 2023.](#)

939 [ANSA, Regione Marche: \[https://www.ansa.it/marche/notizie/2023/11/07/senigalliademolito-ponte-garibaldi-simbolo-\]\(https://www.ansa.it/marche/notizie/2023/11/07/senigalliademolito-ponte-garibaldi-simbolo-dellalluvione-2022\_c834fc28-e7c4-4e8d-9573-0346a0c13560.html\)](#)  
940 [dellalluvione-2022\\_c834fc28-e7c4-4e8d-9573-0346a0c13560.html](#), last access: 27 May 2024 (2023).

941 [Arrighi, C., Brugioni, M., Castelli, F., Franceschini, S., and Mazzanti, B.: Flood risk assessment in art cities: the](#)  
942 [exemplary case of Florence \(Italy\), \*J. Flood Risk Manag.\*, S616, <https://doi.org/10.1111/jfr3.12226>, 31, 2018.](#)

943 [Arrighi, C.: A global scale analysis of river flood risk of UNESCO world heritage sites, \*Frontiers in Water\* 3, 1–12,](#)  
944 [https://doi.org/10.3389/frwa.2021.764459, 2021.](#)

945 [Arrighi, C., Carraresi A., and Castelli, F.: Resilience of art cities to flood risk: a quantitative model based on depth-](#)  
946 [idleness correlation, \*J. Flood Risk Manag.\*, 15, \(2\), 1–15, <https://doi.org/10.1111/jfr3.12794>, 2022.](#)

947 [Arrighi, C., Tanganelli, M., Cristofaro, M.T., Cardinali, V., Marra, A., Castelli F., and De Stefano, M.: Multi-risk](#)  
948 [assessment in a historical city, \*Nat Hazards\*, 119, 1041–1072, <https://doi.org/10.1007/s11069-021-05125-6>, 2023a.](#)

949 [Arrighi, C., Ballio, F., and Simonelli, T.: A GIS-based flood damage index for cultural heritage, \*Int. J. Disaster Risk\*](#)  
950 [Reduc., 90, 103654, <https://doi.org/10.1016/j.ijdr.2023.103654>, 2023b.](#)

951 [AUBAC: <https://webgis.abdac.it/portal/apps/webappviewer/index.html?id=b4f5f37d97e9427c9c2e4ce7e30928f9>, last](#)  
952 [access: 27 May 2024.](#)

953 [Balasbanch, A.T., Abidin, A.R.Z., Ramli, M.Z., Khaleghi, S.J., and Marsono, A.K.: Vulnerability assessment of building](#)  
954 [material against river flood water: case study in Malaysia, in: \*Proceedings of the 2nd International Conference on Civil\*](#)  
955 [& \*Environmental Engineering\*, IOP Conf. Series: Earth and Environmental Science, 476, 012004, doi:10.1088/1755-](#)  
956 [1315/476/1/012004, 2020.](#)

957 [Beven, K.J. and Kirby, M.J.: A physically based variable contributing area model of basin hydrology, \*Hydrological\*](#)  
958 [Science Bulletin, 24, 43–69, <https://doi.org/10.1080/02626667909491834>, 1979.](#)

959 [Brokerhof, A.W., van Leijen, R., and Gersonius, B.: Protecting built heritage against flood: mapping value density on](#)  
960 [flood hazard maps, \*Water\*, 15, 2950, <https://doi.org/10.3390/w15162950>, 2023.](#)

961 [Clini, P., Muñoz-Cádiz, J., Ferretti, U., Jiménez, J.L.D., and Nieto, G.M.: Digital transition for heritage management and](#)  
962 [dissemination: Via Flaminia and Corduba-Emerita, in: \*Proceedings of the 44th International Conference of\*](#)  
963 [Representation Disciplines Teachers, Milano, FrancoAngeli, pp. 2613-2622, doi.org/10.3280/oa-1016-c425, 2023.](#)

964 [COPERNICUS Emergency Management Service: \[https://emergency.copernicus.eu/mapping/list-of-\]\(https://emergency.copernicus.eu/mapping/list-of-components/EMSR634\)](#)  
965 [components/EMSR634](#), last access: 27 May 2024 (2022).

966 [CRED, UNISDR: \[https://www.preventionweb.net/files/46796\\\_cop21weatherdisastersreport2015.pdf\]\(https://www.preventionweb.net/files/46796\_cop21weatherdisastersreport2015.pdf\), last access: 19](#)  
967 [August 2024 \(2015\).](#)

938 [Cuca, B. and Barazzetti, L.: Damages from extreme flooding events to cultural heritage and landscapes: water component](#)  
939 [estimation for Centa River \(Albenga, Italy\). \*Adv. Geosci.\*, 45, 389–395. <https://doi.org/10.5194/adgeo-45-389-2018>,](#)  
940 [2018.](#)  
941 [D.lgs. 22 gennaio 2004, n. 42: \[https://www.normattiva.it/esporta/attoCompleto?atto.dataPubblicazioneGazzetta=2004-\]\(https://www.normattiva.it/esporta/attoCompleto?atto.dataPubblicazioneGazzetta=2004-02-24&atto.codiceRedazionale=004G0066\)](#)  
942 [02-24&atto.codiceRedazionale=004G0066, last access: 27 May 2024 \(2004\).](#)  
943 [Dall'Osso, F., Gonella, M., Gabbianelli, G., Withycombe, G., and Dominey-Howes, D.: A revised \(PTVA\) model for](#)  
944 [assessing the vulnerability of buildings to tsunami damage, \*Nat. Hazards Earth Syst. Sci.\*, 9, 1557–1565,](#)  
945 [https://doi.org/10.5194/nhess-9-1557-2009, 2009.](#)  
946 [De Donatis, M., Lepore, G., Susini, S., Silani, M., Boschi, F., and Savelli, D.: Sistemi informativi geografici e](#)  
947 [modellazione tridimensionale per la geo-archeologia a Senigallia: nuove scoperte e nuove ipotesi, \*Rend. Online Soc.\*](#)  
948 [Geol. Ital.](#), 19, 16–19, <https://api.semanticscholar.org/CorpusID:135458708>, 2012.  
949 [De Donatis, M., Nesci, O., Savelli, D., Pappafico, G.F., and Susini, S.: Geomorphological evolution of the Sena Gallica](#)  
950 [site in the morpho-evolutionary quaternary context of the northern-Marche coastal sector \(Italy\), \*Geosciences\*, 9, 272,](#)  
951 [https://doi.org/10.3390/geosciences9060272, 2019.](#)  
952 [Deschaux, J.: 4 - Flood-related Impacts on cultural heritage, in: \*Floods\*, edited by: Vinet, F., Elsevier, 53-72,](#)  
953 [https://doi.org/10.1016/B978-1-78548-268-7.50004-3, 2017.](#)  
954 [Di Salvo, C., Pennica, F., Ciotoli, G., and Cavinato, G.P.: A GIS-based procedure for preliminary mapping of pluvial](#)  
955 [flood risk at metropolitan scale, \*Environ. Model. Software\*, 107, 64-84, <https://doi.org/10.1016/j.envsoft.2018.05.020>,](#)  
956 [2018.](#)  
957 [Dottori, F., Mentaschi, L., Bianchi, A., Alfieri, L., and Feyen, L.: Cost-effective adaptation strategies to rising river flood](#)  
958 [risk in Europe, \*Nat. Clim. Change\*, 13, 196–202, <https://doi.org/10.1038/s41558-022-01540-0>, 2023.](#)  
959 [Drdáček, M.F.: Impact of floods on heritage structures, \*J. Perform. Constr. Facil.\*, 24, 430–431](#)  
960 [https://doi.org/10.1061/\(ASCE\)CF.1943-5509.0000152, 2010.](#)  
961 [Dutta, D., Wright, W., and Rayment, P.: Synthetic impact response functions for flood vulnerability analysis and](#)  
962 [adaptation measures in coastal zones under changing climatic conditions: a case study in Gippsland coastal region,](#)  
963 [Australia, \*Nat. Hazards\*, 59\(2\):967–986, <https://doi.org/10.1007/s11069-011-9812-x>, 2011.](#)  
964 [ESRI, ArcGIS PRO: release 3.2.2. Redlands, CA: Environmental Systems Research Institute, 2023.](#)  
965 [EU, Directive 2007/60/EC of the European Parliament and of the Council of 23 October 2007 on the Assessment and](#)  
966 [Management of Flood Risks, European Environment Agency: Copenhagen, Denmark, pp. 27–34, 2007.](#)  
967 [Fatorić, S. and Seekamp, E.: Are cultural heritage and resources threatened by climate change? A systematic literature](#)  
968 [review, \*Climatic Change\*, 142\(1–2\), 227–254, <https://doi.org/10.1007/s10584-017-1929-9>, 2017.](#)  
969 [Figueiredo, R., Romão, X., and Paupério, E.: Flood risk assessment of cultural heritage at large spatial scales: framework](#)  
970 [and application to mainland Portugal, \*Journal of Cultural Heritage\*, 43, 163-174,](#)  
971 [https://doi.org/10.1016/j.culher.2019.11.007, 2020.](#)  
972 [Figueiredo, R., Romão, X., and Paupério, E.: Component-based flood vulnerability modelling for cultural heritage](#)  
973 [buildings, \*International Journal of Disaster Risk Reduction\*, 61\(January\), 102323,](#)  
974 [https://doi.org/10.1016/j.ijdr.2021.102323, 2021.](#)  
975 [Galasso, C., Pregnolato, P., and Parisi, F.: A model taxonomy for flood fragility and vulnerability assessment of buildings,](#)  
976 [International Journal of Disaster Risk Reduction, 53, 101985, <https://doi.org/10.1016/j.ijdr.2020.101985>, 2021.](#)

977 [Garrote, J., Díez-Herrero, A., Escudero, C., and García I.: A framework proposal for regional-scale flood-risk assessment](#)  
978 [of cultural heritage sites and application to the Castile and León Region \(Central Spain\), \*Water\*, 12\(2\):329,](#)  
979 <https://doi.org/10.3390/w12020329>, 2020.

980 [GLI ANGELI DELLE TINTE: https://fondoambiente.it/il-fai/grandi-campagne/i-luoghi-del-cuore/comitati/1347](#), last  
981 [access: 27 May 2024 \(2022\).](#)

982 [Godfrey, A., Ciurean, R.L., Van Westen, C.J., Kingma, N.C., and Glade, T.: Assessing vulnerability of buildings to hydro-](#)  
983 [meteorological hazards using an expert based approach—an application in Nehoiu Valley, Romania, \*Int. J. Disaster Risk\*](#)  
984 [Reduct.](#), 13, 229–241, <https://doi.org/10.1016/j.ijdr.2015.06.001>, 2015.

985 [Gschnitzer, T., Gems, B., Mazzorana B., and Aufleger M.: Towards a robust assessment of bridge clogging processes in](#)  
986 [flood risk management, \*Geomorphology\*, 279, 128-140, https://doi.org/10.1016/j.geomorph.2016.11.002](#), 2017.

987 [Historic England: https://historicengland.org.uk/images-books/publications/conservation-principles-sustainable-](#)  
988 [management-historic-environment/](#), last access: 19 August 2024 (2008).

989 [Huijbregts, Z., van Schijndel, J. W. M., Schellen, H. L., and Blades, N.: Hygrothermal modelling of flooding events](#)  
990 [within historic buildings, \*J. Build. Phys.\*, 38\(2\), 170–187, https://doi.org/10.1177/1744259114532613](#), 2014.

991 [Iacobucci, G., Piacentini, D., and Troiani, F.: Enhancing the identification and mapping of fluvial terraces combining](#)  
992 [geomorphological field survey with land-surface quantitative analysis, \*Geosciences\*, 12, 425, https://doi.org/10.3390/](#)  
993 [geosciences12110425](#), 2022.

994 [IPCC: https://www.ipcc.ch/report/sixth-assessment-report-cycle/](#), last access: 19 August 2024 (2023).

995 [Istituto Superiore per la Conservazione ed il Restauro – MiBACT:](#)  
996 <http://vincoliinrete.beniculturali.it/VincoliInRete/vir/bene/listabeni>, last access: 27 May 2024.

997 [Jeggle, T. and Boggero, M.: Post-disaster needs assessment \(PDNA\): lessons from a decade of experience, European](#)  
998 [Commission, GFDRR, UNDP, and the World Bank, <http://hdl.handle.net/10986/30945>, License: CC BY-NC-ND 3.0](#)  
999 [IGO, 2018.](#)

1000 [Kefi, M., Mishra, B.K., Masago, Y., and Fukushi, K.: Analysis of flood damage and influencing factors in urban](#)  
1001 [catchments: case studies in Manila, Philippines, and Jakarta, Indonesia, \*Nat. Hazards\*, 104, 2461–2487,](#)  
1002 <https://doi.org/10.1007/s11069-020-04281-5>, 2020.

1003 [Kreibich, H. and Thieken, A.H.: Assessment of damage caused by high groundwater inundation, \*Water Resour. Res.\*,](#)  
1004 [44:W09409, https://doi.org/10.1029/2007W R0066 21](#), 2008.

1005 [Marín-García, D., Rubio-Gómez-Torga, J., Duarte-Pinheiro, M., and Moyano, J.: Simplified automatic prediction of the](#)  
1006 [level of damage to similar buildings affected by river flood in a specific area, \*Sustain. Cities Soc.\*, 88, 104251,](#)  
1007 <https://doi.org/10.1016/j.scs.2022.104251>, 2023.

1008 [Mark, O., Weesakul, S., Apirumanekul, C., Boonya Aroonnet, S., and Djordjevic, S.: Potential and limitations of 1D](#)  
1009 [modelling of urban flooding, \*J. Hydrol.\*, 299, 284–299, <http://dx.doi.org/10.1016/j.jhydrol.2004.08.014>, 2004.](#)

1010 [Martín-Vide, J.P., Bateman A., Berenguer M., Ferrer-Boix C., Amengual A., Campillo M., Corral C., Llasat M.C., Llasat-](#)  
1011 [Botija M., Gómez-Dueñas S., Marín-Esteve B., Núñez-González F., Prats-Puntí A., Ruiz-Carulla R., and Sosa-Pérez R.:](#)  
1012 [Large wood debris that clogged bridges followed by a sudden release, the 2019 flash flood in Catalonia, \*J. Hydrol. Reg.\*](#)  
1013 [Stud.](#), 47, 101348, <https://doi.org/10.1016/j.ejrh.2023.101348>, 2023.

1014 [Marzeion, B. and Levermann, A.: Loss of cultural world heritage and currently inhabited places to sea-level rise, \*Environ.\*](#)  
1015 [Res. Lett.](#), 9(3), 034001, <https://doi.org/10.1088/1748-9326/9/3/034001>, 2014.

1016 [MASE, Geoportale Nazionale: https://gn.mase.gov.it/portale/distribuzione-dati-pst](#), last access 27 May 2024.

1017 [Mastrorillo, L. and Petitta, M.: Effective infiltration variability in the Umbria-Marche carbonate aquifers of central Italy, \*J. Mediterr. Earth Sci.\*, 2. <https://doi.org/10.3304/JMES.2010.004>, 2014.](#)

1018

1019 [Merz, B., Blöschl, G., Vorogushyn, S., Dottori, F., Aerts, J. C. J. H., Bates, P., Bertola, M., Kemter, M., Kreibich, H.,](#)

1020 [Lall, U. and Macdonald, E.: Causes, impacts and patterns of disastrous river floods. \*Nat. Rev. Earth Environ.\* 2, 592–609.](#)

1021 [doi: 10.1038/s43017-021-00195-3, 2021.](#)

1022 [Molinari, D., Menoni, S., Aronica, G. T., Ballio, F., Berni, N., Pandolfo, C., Stelluti, M., and Minucci, G.: Ex post damage](#)

1023 [assessment: an Italian experience. \*Nat. Hazards Earth Syst. Sci.\*, 14, 901–916, doi:10.5194/nhess-14-901-2014, 2014.](#)

1024 [Momčilović Petronijević, A. and Petronijević, P.: Floods and Their Impact on Cultural Heritage - a Case Study of](#)

1025 [Southern and Eastern Serbia, \*Sustainability\*, 14, 14680. <https://doi.org/10.3390/su142214680>, 2022.](#)

1026 [Moore, I.D., Grayson, R.B., and Ladson, A.R.: Digital terrain modeling: a review of hydrological, geomorphological, and](#)

1027 [biological applications, \*Hydrol. Processes\*, 5, pp. 3-30, <https://doi.org/10.1002/hyp.3360050103>, 1991.](#)

1028 [Pulvirenti, L., Squicciarino, G., Fiori, E., Candela, L., and Puca, S.: Analysis and processing of the COSMO-SkyMed](#)

1029 [second generation images of the 2022 Marche \(Central Italy\) flood, \*Water\*, 15, 1353. <https://doi.org/10.3390/w15071353>,](#)

1030 [2023.](#)

1031 [Ravan, M., Revez, M.J., Pinto, I.V., Brum, P., Birkmann, J.: A vulnerability assessment framework for cultural heritage](#)

1032 [sites: the case of the Roman ruins of Tróia, \*Int. J. Disaster Risk Sci.\*, 14, 26–40, \[https://doi.org/10.1007/s13753-023-\]\(https://doi.org/10.1007/s13753-023-00463-4\)](#)

1033 [00463-4, 2023.](#)

1034 REGIONE MARCHE, ANNALI IDROLOGICI:

1035 [https://www.regione.marche.it/portals/0/Protezione\\_Civile/Manuali%20e%20Studi/annale-parte-1-2021.pdf](https://www.regione.marche.it/portals/0/Protezione_Civile/Manuali%20e%20Studi/annale-parte-1-2021.pdf), last access:

1036 [27 May 2024 \(2021\).](#)

1037 REGIONE MARCHE, RAPPORTO DI EVENTO preliminare:

1038 [https://www.regione.marche.it/portals/0/Protezione\\_Civile/Manuali%20e%20Studi/Rapporto\\_Evento\\_preliminare\\_202](https://www.regione.marche.it/portals/0/Protezione_Civile/Manuali%20e%20Studi/Rapporto_Evento_preliminare_202)

1039 [20915.pdf](#), last access: 27 May 2024 (2022). REGIONE MARCHE, Ambiente: [https://www.regione.marche.it/Regione-](https://www.regione.marche.it/Regione-Utile/Paesaggio-Territorio-Urbanistica/Cartografia)

1040 [Utile/Paesaggio-Territorio-Urbanistica/Cartografia](#), last access: 27 May 2024 (2023).

1041 [Reimann, L., Vafeidis, A.T., Brown, S., Hinkel, J., and Tol, R.S.J.: Mediterranean UNESCO world heritage at risk from](#)

1042 [coastal flooding and erosion due to sea-level rise, \*Nat. Commun.\*, 9\(1\), 4161, \[https://doi.org/10.1038/s41467-018-06645-\]\(https://doi.org/10.1038/s41467-018-06645-9\)](#)

1043 [9, 2018.](#)

1044 [Riley, S.J., DeGloria, S.D., and Elliot, R.: A terrain ruggedness index that quantifies topographic heterogeneity, \*Int. J.\*](#)

1045 [\*Sci.\*, 5\(1–4\):23–27, 1999.](#)

1046 [Romao, X., Paupério, E., Monserrat, O., Rousakis, T., and Montero, P.: Assets at risk and potential impacts: 3.6 - cultural](#)

1047 [heritage, in: \*Science for Disaster Risk Management 2020: Acting Today, Protecting Tomorrow\*, edited by: Casajus Valles,](#)

1048 [A., Marin Ferrer, M., Poljanšek, K., and Clark, I., Publications Office of the European Union, Luxembourg, 503-525, doi:](#)

1049 [10.2760/571085, 2020.](#)

1050 [Romão, X., and Paupério, E.: An indicator for post-disaster economic loss valuation of impacts on cultural heritage, \*Int.\*](#)

1051 [\*J. Arch. Herit.\*, 15\(5\), 678–697, <https://doi.org/10.1080/15583058.2019.1643948>, 2021.](#)

1052 [Sabbioni, C., Brimblecombe, P., Bonazza, A., Grossi, C. M., Harris, I., and Messina, P.: Mapping climate change and](#)

1053 [cultural heritage, in: \*Proceedings of the 7th EC Conference on Safeguarded Cultural Heritage - Understanding and\*](#)

1054 [\*Viability for the Enlarged Europe\*, edited by: Drdacky, M., Prague, Czech Republic, Institute of Theoretical and Applied](#)

1055 [\*Mechanics of the Academy of Sciences of the Czech Republic\*, 119–124, 2007.](#)

1056 [Salazar, L.G.F., Romão, X., and Figueiredo, R.: A hybrid approach for the assessment of flood vulnerability of historic](#)

1057 [constructions and their contents, in: \*Proceedings of the Structural Analysis of Historical Constructions\*, edited by: Endo,](#)

1058 [Y. and Hanazato, T., SAHC 2023, RILEM Bookseries, vol 46., Springer, Cham., https://doi.org/10.1007/978-3-031-](https://doi.org/10.1007/978-3-031-39450-8_91)  
1059 [39450-8\\_91, 2024.](https://doi.org/10.1007/978-3-031-39450-8_91)

1060 [Schlumberger, J., Ferrarin, C., Jonkman, S. N., Diaz Loaiza, M. A., Antonini, A., and Fatorić, S.: Developing a framework](https://doi.org/10.5194/nhess-22-2381-2022)  
1061 [for the assessment of current and future flood risk in Venice, Italy, Nat. Hazards Earth Syst. Sci., 22, 2381–2400,](https://doi.org/10.5194/nhess-22-2381-2022)  
1062 [https://doi.org/10.5194/nhess-22-2381-2022, 2022.](https://doi.org/10.5194/nhess-22-2381-2022)

1063 [Sesana, E., Gagnon, A.S., Ciantelli, C., Cassar, J.A., Hughes, J.J.: Climate change impacts on cultural heritage: A](https://doi.org/10.1002/wcc.710)  
1064 [literature review, WIREs Clim Change, 12:e710. https://doi.org/10.1002/wcc.710, 2021.](https://doi.org/10.1002/wcc.710)

1065 [Shepard, D.: A two-dimensional interpolation function for irregularly-spaced data, in: Proceedings of the 23th ACM](https://doi.org/10.1145/359211)  
1066 [National Conference, New York, NY, USA, 27–29 August 1968, pp. 517–524, 1968.](https://doi.org/10.1145/359211)

1067 [SIRMIP ON-LINE: http://app.protezionecivile.marche.it/sol/indexjs.sol?lang=it, last access: 27 May 2024.](http://app.protezionecivile.marche.it/sol/indexjs.sol?lang=it)

1068 [Smith, D.I.: Flood damage estimation - a review of urban stage-damage curves and loss functions, Water, S.A., 20:231–](https://doi.org/10.1080/00220717.1994.10673338)  
1069 [238, https://hdl.handle.net/10520/AJA03784738\\_1124, 1994.](https://doi.org/10.1080/00220717.1994.10673338)

1070 [Stephenson, V. and D'Ayala, D.: A new approach to flood vulnerability assessment for historic buildings in England, Nat.](https://doi.org/10.5194/nhess-14-1035-2014)  
1071 [Hazards Earth Syst. Sci., 14, 1035–1048, https://doi.org/10.5194/nhess-14-1035-2014, 2014.](https://doi.org/10.5194/nhess-14-1035-2014)

1072 [Storm Chasers Marche: https://www.youtube.com/watch?v=wNFpou4aSg, last access: 27 May 2023 \(2022\).](https://www.youtube.com/watch?v=wNFpou4aSg)

1073 [Sulphur, MARCHE MINING GEOPARK: https://www.museosulphur.it/en/marche-mining-geopark/, last access: 27](https://www.museosulphur.it/en/marche-mining-geopark/)  
1074 [May 2024.](https://www.museosulphur.it/en/marche-mining-geopark/)

1075 [Tarquini, S., Isola, I., Favalli, M., Mazzarini, F., Bisson, M., Pareschi, M.T., and Boschi, E.: TINITALY/01: a new](https://doi.org/10.4401/ag-4424)  
1076 [triangular irregular network of Italy, Annals of Geophysics, https://doi.org/10.4401/ag-4424, 2007.](https://doi.org/10.4401/ag-4424)

1077 [Tarquini S., Isola, I., Favalli, M., Battistini, A., and Dotta, G.: TINITALY, a digital elevation model of Italy with a 10](https://doi.org/10.13127/tinitaly/1.1)  
1078 [meters cell size \(Version 1.1\), Istituto Nazionale di Geofisica e Vulcanologia \(INGV\),](https://doi.org/10.13127/tinitaly/1.1)  
1079 [https://doi.org/10.13127/tinitaly/1.1, 2023.](https://doi.org/10.13127/tinitaly/1.1)

1080 [TGCOM24: https://www.tgcom24.mediaset.it/2022/video/alluvione-marche-a-cantiano-il-ponte-romano-resiste-al-](https://www.tgcom24.mediaset.it/2022/video/alluvione-marche-a-cantiano-il-ponte-romano-resiste-al-disastro_55048806-02k.shtml)  
1081 [disastro\\_55048806-02k.shtml, last access: 27 May 2024 \(2022\).](https://www.tgcom24.mediaset.it/2022/video/alluvione-marche-a-cantiano-il-ponte-romano-resiste-al-disastro_55048806-02k.shtml)

1082 [Trizio, F., Torrijo, F.J., Mileto, C., and Vegas, F.: Flood risk in a heritage city: Alzira as a case study, Water, 13, 1138,](https://doi.org/10.3390/w13091138)  
1083 [https://doi.org/10.3390/w13091138, 2021.](https://doi.org/10.3390/w13091138)

1084 [Vafadari, A., Philip, G., and Jennings, R.P.: Damage assessment and monitoring of cultural heritage places in a disaster](https://doi.org/10.5194/isprs-archives-xlii-2-w5-695-2017)  
1085 [and post-disaster event – a case study of Syria, ISPRS - International Archives of the Photogrammetry, Remote Sensing](https://doi.org/10.5194/isprs-archives-xlii-2-w5-695-2017)  
1086 [and Spatial Information Sciences, 42, 695-701, doi:10.5194/ISPRS-ARCHIVES-XLII-2-W5-695-2017, 2017.](https://doi.org/10.5194/isprs-archives-xlii-2-w5-695-2017)

1087 [Vecvagars, K. and NU. CEPAL. Subsede de México \(eds.\): Valuing damage and losses in cultural assets after a disaster:](https://doi.org/10.1016/j.culher.2014.03.002)  
1088 [concept paper and research options, Naciones Unidas Comisión Económica para América Latina y el Caribe \(CEPAL\),](https://doi.org/10.1016/j.culher.2014.03.002)  
1089 [59 pp., ISBN 9211216117, 2006.](https://doi.org/10.1016/j.culher.2014.03.002)

1090 [Wang, J.-J.: Flood risk maps to cultural heritage: Measures and process, J. Cult. Herit., 16\(2\), 210–220,](https://doi.org/10.1016/j.culher.2014.03.002)  
1091 [https://doi.org/10.1016/j.culher.2014.03.002, 2015.](https://doi.org/10.1016/j.culher.2014.03.002)

1092 [Willis, K.G.: The use of stated preference methods to value cultural heritage, in: Handbook of the Economics of Art and](https://doi.org/10.1016/B978-0-444-53776-8.00007-6)  
1093 [Culture, edited by: Ginsburgh, V.A., and Throsby D., Elsevier, 145-181, https://doi.org/10.1016/B978-0-444-53776-](https://doi.org/10.1016/B978-0-444-53776-8.00007-6)  
1094 [8.00007-6, 2014.](https://doi.org/10.1016/B978-0-444-53776-8.00007-6)

1095 [World Events News: https://www.youtube.com/watch?v=HjOYO-GS0dM, last access: 27 May 2024 \(2022\).](https://www.youtube.com/watch?v=HjOYO-GS0dM)

1096 [Zhang, S.-N., Ruan, W.-Q., Li, Y.-Q., Xiao, H.: Cultural distortion risks at heritage sites: scale development and](https://doi.org/10.1016/j.tourman.2023.104860)  
1097 [validation, Tourism Management, 102, 104860, https://doi.org/10.1016/j.tourman.2023.104860, 2024.](https://doi.org/10.1016/j.tourman.2023.104860)

1098 [Zugliani, D., Ataieyan, A., Rocco, R., Betemps, N., Ropele, P., Rosatti, G.: Bridge obstruction caused by debris flow: a](#)  
1099 [practical procedure for its management in debris-flow simulations, in: Proceedings of the 8th International Conference](#)  
1100 [on Debris Flow Hazard Mitigation \(DFHM8\), Turin, Italy, 26-29 June 2023, 05031,](#)  
1101 [https://doi.org/10.1051/e3sconf/202341505031, 2023.](https://doi.org/10.1051/e3sconf/202341505031)

**ha eliminato:** Adeyemo, O.J., Maksimovic, C., Booyan – Aaronnet, S., Leitao, J., Butler, D., Makropoulos, C., 2008. Sensitivity analysis of surface runoff generation for Pluvial Urban Flooding. In: 11th International Conference on Urban Drainage, Edinburgh, Scotland, UK, 2008.¶  
Al-Kindi, K.M. and Alabri, Z. Investigating the Role of the Key Conditioning Factors in Flood Susceptibility Mapping Through Machine Learning Approaches. *Earth Syst Environ* 8, 63–81 (2024). <https://doi.org/10.1007/s41748-023-00369-7>.¶  
Alexandrakis, G.; Manasakis, C.; Kampanis, N.A. Economic and Societal Impacts on Cultural Heritage Sites, Resulting from Natural Effects and Climate Change. *Heritage* 2019, 2, 279-305. <https://doi.org/10.3390/heritage2010019>.¶  
Amaddii, M.; Rosatti, G.; Zugliani, D.; Marzini, L.; Disperati, L. Back-Analysis of the Abbadia San Salvatore (Mt. Amiata, Italy) Debris Flow of 27–28 July 2019: An Integrated Multidisciplinary Approach to a Challenging Case Study. *Geosciences* 2022, 12, 385. <https://doi.org/10.3390/geosciences12100385>.¶  
Amaddii M., Rosatti G., Zugliani D., Marzini L. & Disperati L. (2023) - Modelling stony debris flows involving culverted streams: the Abbadia San Salvatore case (Mt. Amiata, Italy). *Rend. Online Soc. Geol.It.*, 61, 108-115, <https://doi.org/10.3301/ROL.2023.55>.¶  
Anderson, K. The impact of increased flooding caused by climate change on heritage in England and North Wales, and possible preventative measures: what could/should be done?. *Built Heritage* 7, 7 (2023). <https://doi.org/10.1186/s43238-023-00087-z>.¶  
ANSA, Regione Marche: [https://www.ansa.it/marche/notizie/2023/11/07/senigalliademolito-ponte-garibaldi-simbolo-dellalluvione-2022\\_c834fc28-e7c4-4e8d-9573-0346a0c13560.html](https://www.ansa.it/marche/notizie/2023/11/07/senigalliademolito-ponte-garibaldi-simbolo-dellalluvione-2022_c834fc28-e7c4-4e8d-9573-0346a0c13560.html), last access: 27 May 2024 (2023).¶  
Arrighi, C.; Brugioni, M.; Castelli, F.; Franceschini, S.; Mazzanti, B. Flood risk assessment in art cities: the exemplary case of Florence (Italy). *J. Flood Risk Manage.* (2018), S616, <https://doi.org/10.1111/jfr3.12226>, 31.¶  
Arrighi, C. A global scale analysis of river flood risk of UNESCO world heritage sites, *Frontiers in Water* 3 (2021) 1–12, <https://doi.org/10.3389/frwa.2021.764459>, December.¶  
Arrighi, C.; Carraresi A.; Castelli, F. Resilience of art cities to flood risk: a quantitative model based on depth-idleness correlation, *J. Flood Risk Manage.* 15 (2) (2022) 1–15, <https://doi.org/10.1111/jfr3.12794>.¶  
Arrighi, C.; Tanganelli, M.; Cristofaro, M.T. et al. Multi-risk assessment in a historical city. *Nat Hazards* 119, 1041–1072 (2023a). <https://doi.org/10.1007/s11069-021-05125-6>.¶  
Arrighi, C.; Ballio, F.; Simonelli, T. 2023b. A GIS-based flood damage index for cultural heritage. *International Journal of Disaster Risk Reduction* 90, 103654. <https://doi.org/10.1016/j.ijdrr.2023.103654>.¶  
AUBAC: <https://webgis.abdac.it/portal/apps/webappviewer/index.html?id=b4f5f37d97e9427c9c2e4ce7c30928f9>, last access: 27 May 2024.¶  
Balasbaneh, A.T. et al 2020 IOP Conf. Ser.: Earth Environ. Sci. 476 012004 DOI 10.1088/1755-1315/476/1/012004.¶  
Beven, K.J. and Kirby, M.J. 1979. A physically based variable contributing area model of basin hydrology. *Hydrological Science Bulletin* 24, 43–69.¶  
Brokerhof, A.W.; van Leijen, R.; Gersonius, B. Protecting Built Heritage against Flood: Mapping Value Density on Flood Hazard Maps. *Water* 2023, 15, 2950. <https://doi.org/10.3390/w15162950>.¶  
Clini, P.; Muñoz-Cádiz, J.; Ferretti, U.; Jiménez, J.L.D. Nieto, G.M. (2023). Digital Transition for Heritage ... [1]